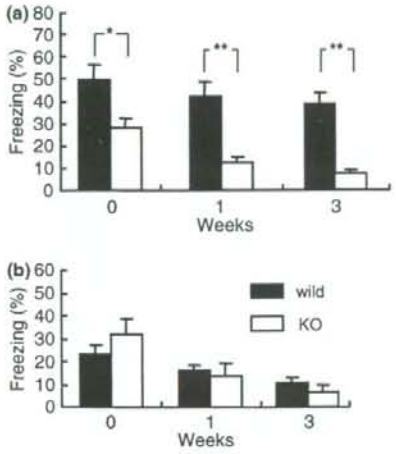

Fig. 1 Contextual (a) and cued (b) fear-conditioning tests in neurotensin receptor subtype 2 (Ntsr2)-deficient (open bar, KO) and wild-type (filled bar) mice. The rate of freezing (%) was calculated to indicate fear memory. The values shown are means ± SEM ($n = 9$). $^{*}p < 0.05$ and $^{**}p < 0.01$ versus control are considered as significant using the unpaired Student's *t*-test.

of wild-type mice at 0, 1, 3, and 6 weeks after conditioning (all $p > 0.05$, Fig. 1b).

To investigate the freezing response at an early stage, contextual fear-conditioning tests were performed at 1 and 5 h after conditioning. The freezing response in the contextual test at 1 h after conditioning was significantly reduced in Ntsr2-deficient mice compared with that of wild-type mice (wild type: 46.5 ± 2.9%, $n = 9$; deficient: 31.9 ± 5.4%, $n = 9$; $p < 0.05$, Fig. 2). At 5 h after conditioning, the freezing response of Ntsr2-deficient mice was slightly reduced, but not significantly, compared with that of wild-type mice (wild type: 28.5 ± 7.3%, $n = 9$; deficient:

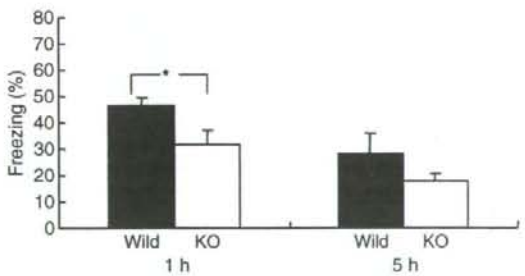

Fig. 2 Contextual fear-conditioning test performed at 1 and 5 h immediately after conditioning, in neurotensin receptor subtype 2 (Ntsr2)-deficient (open bar, KO) and wild-type (filled bar) mice. The rate of freezing (%) was calculated to indicate fear memory. The values shown are means ± SEM ($n = 10$). $^{*}p < 0.05$ versus control are considered as significant using the unpaired Student's *t*-test.

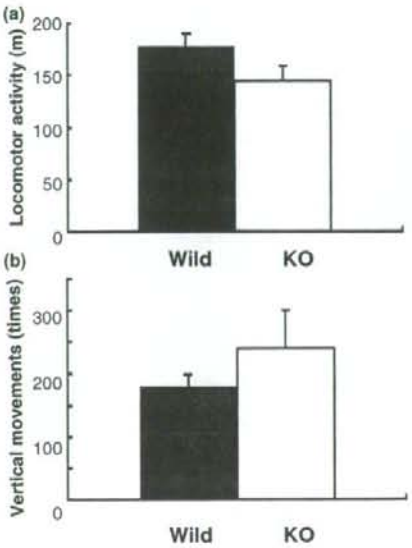

Fig. 3 Total locomotor activity (a) and vertical movements (b) in neurotensin receptor subtype 2 (Ntsr2)-deficient (open bar, KO) and wild-type (filled bar) mice. The values shown are means ± SEM ($n = 8$).

18.0 ± 2.5%, $n = 9$; Fig. 2). These results suggest that Ntsr2 is involved in contextual fear memory.

Spontaneous activity

The decreased freezing responses of Ntsr2-deficient mice in the contextual fear-conditioning test may be caused by the decrease in spontaneous activities. With the spontaneous activity test, there were no differences between wild-type and Ntsr2-deficient mice in locomotor activity (wild type: 17759.4 ± 1278.1 cm, $n = 8$; deficient: 14469.2 ± 1390.7 cm, $n = 8$, $p > 0.05$, Fig. 3a) and vertical movements (wild type: 180.3 ± 17.8, $n = 8$; deficient: 240.1 ± 59.9, $n = 8$, $p > 0.05$, Fig. 3b). Stereotypic movements in Ntsr2-deficient mice were similar to that in wild-type mice (wild type: 6717.4 ± 271.5, $n = 8$; deficient: 7012 ± 334.9, $n = 8$, $p > 0.05$). These results suggest that spontaneous activity was not altered in Ntsr2-deficient mice.

Shock sensitivity

Recently, we reported that Ntsr2-deficient mice showed altered thermal nociception in the hot plate test (Maeno *et al.* 2004). To confirm if these mice percept the electrical shock, we measured electrical-shock sensitivity in Ntsr2-deficient and wild-type mice. There was no difference in shock sensitivity between Ntsr2-deficient and wild-type mice (wild type: 52.0 ± 3.9 μA, $n = 8$; deficient: 45.1 ± 3.7 μA, $n = 9$; $p > 0.05$, Fig. 4). These results suggest that deficiency of Ntsr2 is not responsible for electrical shock sensitivity.

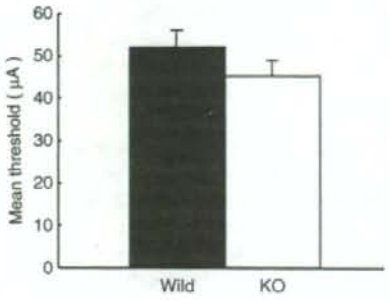

Fig. 4 Shock sensitivity in neurotensin receptor subtype 2 (Ntsr2)-deficient (open bar, KO) and wild-type (filled bar) mice. The values shown are mean thresholds (μA) ± SEM (n = 9).

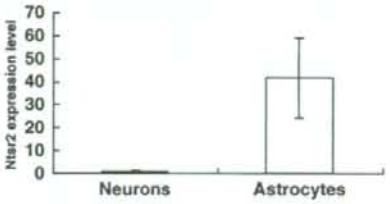

Fig. 5 Neurotensin receptor subtype 2 (Ntsr2) mRNA expression levels in neurons (filled bar) and astrocytes (open bar) in C57BL/6J mice brain. The values are the amount of expression levels of quantitative RT-PCR products ± SEM (n = 4).

Ntsr2 gene expression in primary cultured cells

The distribution of Ntsr2 mRNA has been observed in the mouse brain (Sarret *et al.* 1998; Walker *et al.* 1998). However, the cells that express Ntsr2 mRNA have not been clearly characterized. To examine the subpopulation of cells expressing Ntsr2 in the mouse brain, we performed real-time quantitative RT-PCR on total RNA extracted from primary-cultured astrocytes, neurons and oligodendrocytes.

Neurotensin receptor subtype 2 mRNA was predominantly expressed in cultured astrocytes (Fig. 5), but only weakly expressed in cultured neurons. The amount of Ntsr2 mRNA expression in astrocytes was about 40 times that in neurons. Furthermore, Ntsr2 mRNA was not expressed in rat oligodendrocytes (CG4 OL) (data not shown). These results suggest that Ntsr2 mRNA is mainly expressed in astrocytes *in vitro*.

Ntsr2 gene expression in the mouse brain

To confirm the distribution of Ntsr2 mRNA in the mouse brain, ISH was performed with ^{35}S-labeled cRNA probe. As previously reported, moderate hybridization signals for Ntsr2 anti-sense probe were observed diffusely throughout the brain, including the cortex, thalamus, hypothalamus, and hippocampus. Although hybridization signals were observed diffusely throughout the brain, intense signals were observed

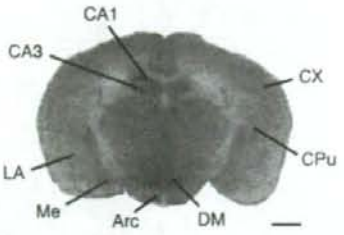

Fig. 6 Neurotensin receptor subtype 2 (Ntsr2) gene expression in the mouse brain. An autoradiogram of a representative coronal section hybridized with a ^{35}S-labeled anti-sense cRNA probe for Ntsr2 is shown. Arc, arcuate nucleus; CA1, field CA1 of Ammon's horn; CA3, field CA3 of Ammon's horn; CPu, caudate–putamen; CX, cortex; DM, dorsomedial hypothalamic nucleus; LA, lateral amygdaloid nucleus; Me, medial amygdaloid nucleus. Scale bar indicates 1 mm.

in the hypothalamic region including pre-optic nuclei and hypothalamic nuclei, pyramidal cell layer of Ammon's horn, and globus pallidus (Fig. 6). By contrast, very weak signals were observed in the internal capsule and fimbria hippocampus. No hybridization signal above background was observed with the Ntsr2 sense probe.

Characterization of cells expressing Ntsr2 mRNA in the mouse brain

To characterize the cells expressing Ntsr2 mRNA, sections were hybridized with DIG-labeled anti-sense or sense Ntsr2 cRNA probes. The pattern of hybridization with a DIG-labeled probe was consistent with that of signals obtained by using a ^{35}S-labeled probe. Hybridized sections were then immunostained with cell type-specific antibodies, including the neuronal nuclei-specific anti-MAP2 antibody and the astrocyte-specific anti-GFAP antibody (Fig. 7). In the hypothalamus and globus pallidus, many Ntsr2 mRNA positive cells were stained with anti-GFAP antibody (Fig. 7f). In the Ammon's horn, Ntsr2 mRNA was expressed in GFAP-immunopositive cells in the oriens layer and radiatum layer, whereas cells expressing Ntsr2 mRNA were stained with anti-MAP2 antibody in the pyramidal cell layer (Fig. 7a–e). These results suggest that, *in vivo*, Ntsr2 mRNA is dominantly expressed in astrocytes, whereas gene expression of Ntsr2 was not as prominent in neurons.

Discussion

Neurotensin has various biological activities, including modulation of feeding and learning behaviors and anti-nociception. Among its various functions, Ntsr1 mediates learning and memory. For example, rats treated with the Ntsr1-specific antagonist, SR 48692, make more working memory errors in spatial learning (Tirado-Santiago *et al.* 2006). In mice, SR 48692 significantly modifies the risk assessment aspect of defensive behavior (Griebel *et al.*

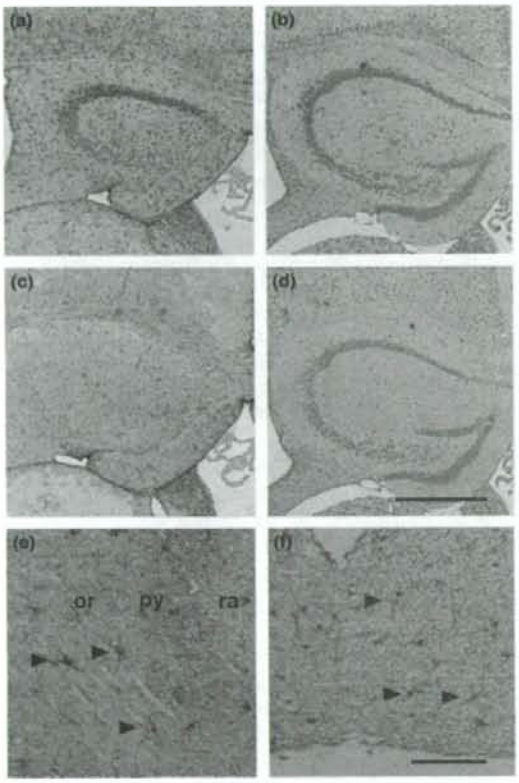

Fig. 7 A combination of *in situ* hybridization (ISH) for neurotensin receptor subtype 2 (Ntsr2) and IHC for glial fibrillary acidic protein (GFAP) or microtubule associated protein-2 (MAP2) in the hippocampus (a–e) and hypothalamus (f). Expression of Ntsr2 mRNA was demonstrated by ISH using digoxigenin (DIG)-labeled anti-sense (a, b, e, and f) or sense (c, and d) probes. In addition to ISH, sections were stained with anti-GFAP antibody (a, c, e, and f), or anti-MAP2 antibody (b, and d). Arrowheads show Ntsr2 gene expression in GFAP-positive cells. or, oriens layer of Ammon's horn; py, pyramidal cell layer of Ammon's horn; ra, radiatum layer of Ammon's horn. Scale bars indicate 500 μm (d) and 100 μm (f).

2001). In contrast to Ntsr1, the biological effects of Ntsr2 on learning and memory have not been reported, although the spinal nociceptive effects of Ntsr2 have been studied well (Maeno *et al.* 2004). In this study, we showed that the freezing response of Ntsr2-deficient mice during contextual fear-conditioning test was decreased compared with wild-type mice. Recently, we reported that the administration of Ntsr2 agonist, β-LT, promotes the extinction of cued fear memory, but not affects the contextual fear conditioning (Yamauchi *et al.* 2006). β-LT has affinity to Ntsr2, but it also binds to Ntsr1 as well. Indeed we reported that ileum-contracting activity of β-LT is mediated by Ntsr1 (Yamauchi *et al.* 2003). In addition, the effects of β-LT on fear-conditioning test were not blocked by Ntsr2 antagonist levocavastine in our previous study. These findings suggest that the effects of β-LT on the fear memory might not be mediated by Ntsr2 only.

Fear memory, examined by the fear-conditioning test, is comprised of three different stages of acquisition, consolidation, and extinction (Sotres-Bayon *et al.* 2006). During the acquisition stage, fear memory for the context and shock is established. During conditioning, there was no difference in freezing behavior between Ntsr2-deficient and wild-type mice, suggesting that acquisition of fear memory is not altered in Ntsr2-deficient mice. In the consolidation stage that comes after the acquisition stage, the fear memory is consolidated when the mouse is returned to its homecage (Abel and Lattal 2001). In the present study, a significant decrease in freezing response was observed in Ntsr2-deficient mice compared with that of wild-type mice at the first exposure to the context (24 or 1 h). These results indicate that Ntsr2 may be involved in the consolidation processes of fear memory. After consolidation, fear memory becomes labile when the animal is exposed again to the conditioning context (retrieval), where memories for the context and shock are associated. During retrieval, the fear memory becomes either reconsolidated or extinct. In general, a short-term exposure to the context leads to reconsolidation, whereas a longer exposure leads to extinction by producing new memory of context without shock (Abel and Lattal 2001; Suzuki *et al.* 2004; Zushida *et al.* 2007). In wild-type mice, freezing ratios to context decreased gradually with time but not significant. On the other hand, in Ntsr2-deficient mice, freezing responses were significantly reduced after second exposure to the context at 1, 3, and 6 weeks after conditioning compared with the first exposure to the contextual. This suggests that Ntsr2 may modulate the formation of extinction learning.

Dopamine (DA) is one of the most important neurotransmitters in the amygdala that plays important roles involved in the mechanisms of fear and anxiety. By activating DA D_1 receptor subtype, a potentiation of conditioned fear responses is introduced. An inhibitory action on conditioned fear may be mediated via the D_2 receptor (Pezze and Feldon 2004). Associations between NT and DA have been well investigated (Binder *et al.* 2001; St-Gelais *et al.* 2006). In many brain regions, NT increases the firing rate of DAergic neurons and has a depolarizing effect. These responses induced by NT are mediated at least in part by Ntsr1 (St-Gelais *et al.* 2006). Although at present the neurotransmitter systems that interact with Ntsr2 have not been well investigated, Ntsr2 may modulate fear memory via D_1 and/or D_2 receptors.

We showed that Ntsr2 gene expression was more predominant in primary astrocyte cultures compared with that in primary neuron cultures. To confirm the purity of

astrocytes in the primary astrocyte cultures, immunocytochemistry was performed (data not shown). In the primary astrocyte culture, more than 95% of cultured cells were stained with the anti-GFAP antibody and few cells were stained with the anti-MAP2 antibody or antibodies for other glial cells such as microglia or oligodendrocytes (data not shown). Nouel *et al.* (1999) reported that, of the two forms of Ntsr2, the full-length form is expressed in astrocytes in the rat brain. In fact, we obtained similar results in cultures from mouse brain (data not shown). In addition to *in vivo* studies, we presented the finding that Ntsr2 mRNA is diffusely expressed throughout the mouse brain, which is in good agreement with earlier studies (Sarret *et al.* 1998; Walker *et al.* 1998). By a combination of ISH and IHC, we showed that Ntsr2 mRNA is expressed dominantly in astrocytes in the regions where we observed. By contrast, in the pyramidal cell layer of Ammon's horn, Ntsr2 mRNA was co-localized with MAP2 immunostaining. This finding indicates that in the layer where neurons packed densely like pyramidal cell layer, Ntsr2 gene is apparently expressed higher level in MAP2 positive cells. Sarret *et al.* (2003) reported that Ntsr2-like immunoreactivity is broadly distributed throughout the rat brain, using an N-terminal-specific anti-Ntsr2 antibody. However, no Ntsr2 signal was observed in astrocytes of rat brain, as confirmed by double immunostaining for the astrocyte marker, calcium-binding protein S100β. These disparities may be caused by a difference in the sensitivity of IHC and ISH techniques, and/or a difference that may exist between rat and mouse.

Astrocytes are traditionally thought to provide physical and structural support for neurons. Recently, many investigators have reported that astrocytes play an important role in the central nervous system (Miller 2005). For example, mice devoid of S100β showed enhanced long-term potentiation in the hippocampal CA1 region, suggesting that S100β secreted from astrocytes may modulate a signal cascade involved in neuronal synaptic plasticity (Nishiyama *et al.* 2002). On the other hand, the importance of astrocytic receptors, especially GPCRs, has not been well investigated. Ntsr2 is a member of a GPCR superfamily that is one of the largest classes of receptors in mammalian genomes. GPCRs mediate diverse physiological functions and are the target of more than 50% of all clinical drugs (Lundstrom 2006). Our findings demonstrate the possibility that GPCRs expressed in astrocytes may play an important role in the modulation of higher brain functions such as emotion and fear.

Regarding the involvement of astrocytes in fear memory, there is a report that suggests the involvement of astrocytes in fear-memory formation. Mei *et al.* (2005) reported gene expression profiles in hippocampus of mouse brain after fear conditioning. After fear conditioning, gene expression of phosphoprotein enriched in astrocytes 15 which blocks extracellular signal-regulated kinase-dependent transcription and proliferation was shown to be decreased. Besides, gene expression of glutamine synthetase which is expressed in astrocytes specifically was increased. These observations suggest that astrocytes may be involved in fear memory formation.

Antonelli *et al.* (2002, 2004) reported that NT enhances glutamate release and modifies the function of glutamate receptors. In addition, astrocytes can release glutamate in a calcium-dependent manner to activate *N*-methyl-D-aspartate and α-amino-3-hydoxy-5-methyl-4-isoxazole propionate receptors expressed in adjacent neurons, and modulate synaptic transmission (Parpura and Haydon 2000). These observations raise the possibility of physiological interaction between glutamate and the NT/Ntsr2 system.

Furthermore, in addition to the alterations seen in Ntsr2-deficient mice, Ntsr1-deficient mice show alterations of long-term potentiation in the amygdala which plays a critical role in emotional learning and social cognition (T. Amano *et al.* unpublished data). This finding suggests that Ntsr1-deficient mice may have emotional disorders, such as those involving fear memory. Our observation is the first finding that the NT/NTR system may have an important role in modulating emotional behavior including fear memory.

Acknowledgements

We thank Dr Santo-Yamada and Mr Sato for helping with the animal behavior tests, Dr Zushida for helpful suggestions, Dr Yamada for statistical analysis, Ms Fujita and Ms Yamamoto for breeding the mice, and Mr Takagaki for editing of the manuscript. We thank Drs K. Ikenaka and A. Espinosa de los Monteros for providing CG4 cells. This work was supported by research grants from the Ministry of Health, Labor and Welfare of Japan, the Ministry of Education, Culture, Sports, Science and Technology of Japan, and CREST, the Japan Science and Technology Agency.

References

Abel T. and Lattal K. M. (2001) Molecular mechanisms of memory acquisition, consolidation and retrieval. *Curr. Opin. Neurobiol.* **11**, 180–187.

Antonelli T., Tomasini M. C., Finetti S., Giardino L., Calza L., Fuxe K., Soubrie P., Tanganelli S. and Ferraro L. (2002) Neurotensin enhances glutamate excitotoxicity in mesencephalic neurons in primary culture. *J. Neurosci. Res.* **70**, 766–773.

Antonelli T., Ferraro L., Fuxe K., Finetti S., Fournier J., Tanganelli S., De Mattei M. and Tomasini M. C. (2004) Neurotensin enhances endogenous extracellular glutamate levels in primary cultures of rat cortical neurons: involvement of neurotensin receptor in NMDA induced excitotoxicity. *Cereb. Cortex* **14**, 466–473.

Binder E. B., Kinkead B., Owens M. J. and Nemeroff C. B. (2001) Neurotensin and dopamine interactions. *Pharmacol. Rev.* **53**, 453–486.

Botto J. M., Sarret P., Vincent J. P. and Mazella J. (1997) Identification and expression of a variant isoform of the levocabastine-sensitive neurotensin receptor in the mouse central nervous system. *FEBS Lett.* **400**, 211–214.

Carraway R. and Leeman S. E. (1973) The isolation of a new hypotensive peptide, neurotensin, from bovine hypothalami. *J. Biol. Chem.* **248**, 6854–6861.

Griebel G., Moindrot N., Aliaga C., Simiand J. and Soubrie P. (2001) Characterization of the profile of neurokinin-2 and neurotensin receptor antagonists in the mouse defense test battery. *Neurosci. Biobehav. Rev.* **25**, 619–626.

Holsboer F. (2003) The role of peptides in treatment of psychiatric disorders. *J. Neural Transm. Suppl.* **64**, 17–34.

Leonetti M., Brun P., Clerget M., Steinberg R., Soubrie P., Renaud B. and Suaud-Chagny M. F. (2004) Specific involvement of neurotensin type 1 receptor in the neurotensin – mediated *in vivo* dopamine efflux using knock-out mice. *J. Neurochem.* **89**, 1–6.

Lundstrom K. (2006) Latest development in drug discovery on G protein-coupled receptors. *Curr. Protein Pept. Sci.* 7, 465–470.

Maeno H., Yamada K., Santo-Yamada Y. *et al.* (2004) Comparison of mice deficient in the high- and low-affinity neurotensin receptors, Ntsr1 or Ntsr 2, reveals a novel function for Ntsr2 in thermal nociception. *Brain Res.* **998**, 122–129.

Mazella J., Botto J. M., Guillemare E., Coppola T., Sarret P. and Vincent J. P. (1996) Structure, functional expression, and cerebral localization of the levocabastine-sensitive neurotensin/neuromedin N receptor from mouse brain. *J. Neurosci.* **16**, 5613–5620.

Mazella J., Zsurger N., Navarro V. *et al.* (1998) The 100-kDa neurotensin receptor is gp95/sortilin, a non-G-protein-coupled receptor. *J. Biol. Chem.* **273**, 26273–26276.

Mei B., Li C., Dong S., Jiang C. H., Wang H. and Hu Y. (2005) Distinct gene expression profiles in hippocampus and amygdala after fear conditioning. *Brain Res. Bull.* **67**, 1–12.

Miller G. (2005) The dark side of glia. *Science* **308**, 778–781.

Nishiyama H., Knopfel T., Endo S. and Itohara S. (2002) Glial protein S100B modulates long-term neuronal synaptic plasticity. *Proc. Natl Acad. Sci. USA* **99**, 4037–4042.

Nouel D., Faure M. P., St. Pierre J. A., Alonso R., Quirion R. and Beaudet A. (1997) Differential binding profile and internalization process of neurotensin via neuronal and glial receptors. *J. Neurosci.* **17**, 1795–1803.

Nouel D., Sarret P., Vincent J. P., Mazella J. and Beaudet A. (1999) Pharmacological, molecular and functional characterization of glial neurotensin receptors. *Neuroscience* **94**, 1189–1197.

Okabe S., Vicario-Abejon C., Segal M. and McKay R. D. (1998) Survival and synaptogenesis of hippocampal neurons without NMDA receptor function in culture. *Eur. J. Neurosci.* **10**, 2192–2198.

Parpura V. and Haydon P. G. (2000) Physiological astrocytic calcium levels stimulate glutamate release to modulate adjacent neurons. *Proc. Natl Acad. Sci. USA* **97**, 8629–8634.

Pettibone D. J., Hess J. F., Hey P. J. *et al.* (2002) The effects of deleting the mouse neurotensin receptor NTR1 on central and peripheral responses to neurotensin. *J. Pharmacol. Exp. Ther.* **300**, 305–313.

Pezze M. A. and Feldon J. (2004) Mesolimbic dopaminergic pathways in fear conditioning. *Prog. Neurobiol.* **74**, 301–320.

Remaury A., Vita N., Gendreau S. *et al.* (2002) Targeted inactivation of the neurotensin type 1 receptor reveals its role in body temperature control and feeding behavior but not in analgesia. *Brain Res.* **953**, 63–72.

Rowe W., Viau V., Meaney M. J. and Quirion R. (1995) Stimulation of CRH-mediated ACTH secretion by central administration of neurotensin: evidence for the participation of the paraventricular nucleus. *J. Neuroendocrinol.* **7**, 109–117.

Sarret P., Beaudet A., Vincent J. P. and Mazella J. (1998) Regional and cellular distribution of low affinity neurotensin receptor mRNA in adult and developing mouse brain. *J. Comp. Neurol.* **394**, 344–356.

Sarret P., Perron A., Stroh T. and Beaudet A. (2003) Immunohistochemical distribution of NTS2 neurotensin receptors in the rat central nervous System. *J. Comp. Neurol.* **461**, 520–538.

Sotres-Bayon F., Cain C. K. and LeDoux J. E. (2006) Brain mechanisms of fear extinction: historical perspectives on the contribution of prefrontal cortex. *Biol. Psychiatry* **60**, 329–336.

St-Gelais F., Jomphe C. and Trudeau L. E. (2006) The role of neurotensin in central nervous system pathophysiology: What is the evidence? *J. Psychiatry Neurosci.* **31**, 229–245.

Suzuki A., Josselyn S. A., Frankland P. W., Masushige S., Silva A. J. and Kida S. (2004) Memory reconsolidation and extinction have distinct temporal and biochemical signatures. *J. Neurosci.* **24**, 4787–4795.

Tanaka K., Masu M. and Nakanishi S. (1990) Structure and functional expression of the cloned rat neurotensin receptor. *Neuron* **4**, 847–854.

Tirado-Santiago G., Lazaro-Munoz G., Rodriguez-Gonzalez V. and Maldonado-Vlaar C. S. (2006) Microinfusions of neurotensin antagonist SR48692 within the nucleus accumbens core impair spatial learning in rats. *Behav. Neurosci.* **120**, 1093–1102.

Walker N., Lepee-Lorgeoux I., Fournier J., Betancur C., Rostene W., Ferrara P. and Caput D. (1998) Tissue distribution and cellular localization of the levocabastine-sensitive neurotensin receptor mRNA in adult rat brain. *Mol. Brain Res.* **57**, 193–200.

Yamada K., Ohki-Hamazaki H. and Wada K. (2000) Differential effects of social isolation upon body weight, food consumption, and responsiveness to novel and social environment in bombesin receptor subtype-3 (BRS-3) deficient mice. *Physiol. Behav.* **68**, 555–561.

Yamada K., Santo-Yamada Y. and Wada K. (2003) Stress-induced impairment of inhibitory avoidance learning in female neuromedin B receptor-deficient mice. *Physiol. Behav.* **78**, 303–309.

Yamauchi R., Usui H., Yunden J., Takenaka Y., Tani F. and Yoshikawa M. (2003) Characterization of β-lactotensin, a bioactive peptide derived from bovine β-lactoglobulin, as a neurotensin agonist. *Biosci. Biotechnol. Biochem.* **67**, 940–943.

Yamauchi R., Wada E., Yamada D., Yoshikawa M. and Wada K. (2006) Effect of β-lactotensin on acute stress and fear memory. *Peptides* **27**, 3176–3182.

Yonemasu T., Nakahira K., Okumura S., Kagawa T., Espinosa de los Monteros A., de Vellis J. and Ikenaka K. (1998) Proximal promoter region is sufficient to regulate tissue-specific expression of UDP-galactose: ceramide galactosyltransferase gene. *J. Neurosci. Res.* **52**, 757–765.

Zushida K., Sakurai M., Wada K. and Sekiguchi M. (2007) Facilitation of extinction learning for contextual fear memory by PEPA: a potentiator of AMPA receptors. *J. Neurosci.* **27**, 158–166.

Gene 432 (2009) 60–66

Contents lists available at ScienceDirect

Gene

journal homepage: www.elsevier.com/locate/gene

Molecular cloning and characterization of the common marmoset huntingtin gene

Hirohiko Hohjoh [a,*], Hirofumi Akari [b], Yuko Fujiwara [a,c], Yoshiko Tamura [a], Hirohisa Hirai [d], Keiji Wada [c]

[a] Department of Molecular Genetics, National Institute of Neuroscience, NCNP, 4-1-1 Ogawahigashi, Kodaira, Tokyo 187-8502, Japan
[b] Laboratory of Disease Control, Tsukuba Primate Research Center, National Institute of Biomedical Innovation, Tsukuba, Ibaraki, Japan
[c] Department of Degenerative Neurological Diseases, National Institute of Neuroscience, NCNP, Kodaira, Tokyo, Japan
[d] Primate Research Institute, Kyoto University, Inuyama, Aichi, Japan

ARTICLE INFO

Article history:
Received 24 July 2008
Received in revised form 4 November 2008
Accepted 5 November 2008
Available online 24 November 2008

Received by M. Di Giulio

Keywords:
Common marmoset
Huntingtin
Gene silencing
Immortalized cell line

ABSTRACT

We report here for the first time the isolation and identification of the common marmoset (*Callithrix jacchus*) *huntingtin* (*Htt*) gene, whose ortholog in humans is known to be related to Huntington's disease (HD). A 9396 nucleotide complementary DNA (cDNA) carrying the putative full-length open reading frame of the marmoset *Htt* gene was identified, and highly conserved nucleotide and amino acid sequences among primates were observed. Based on this data and using tools evaluated for the detection of the marmoset *Htt* gene, we have demonstrated gene silencing against the expression of endogenous *Htt* gene in immortalized common marmoset mononuclear cells by means of RNA interference (RNAi). Taken together, the data presented here may assist us in realizing a non-human primate HD model with the common marmoset.

1. Introduction

Huntington's disease (HD) is an autosomal dominant neurodegenerative disease characterized by progressive and selective neural cell death associated with choreic movement and dementia (Walker, 2007). The responsible gene for HD, the huntingtin (Htt) gene, has been identified on chromosome 4q16.3 (Gusella et al., 1983; Gilliam et al., 1987), and an aberrant length of a CAG triplet repeat in exon 1, followed by expanded tracts of polyglutamine in the Htt polypeptide, is greatly involved in the onset of HD (Huntington's-Disease, 1993). Although the molecular mechanisms of either normal or aberrant Htt protein are still poorly understood, HD model animals (Mangiarini et al., 1996; Kazemi-Esfarjani and Benzer, 2000; von Horsten et al., 2003) and cells (Lunkes and Mandel, 1998) for understanding the pathogenesis of HD and developing therapies have been established by means of genetic engineering based on the genetic information of *Htt*. The use of an animal model that is closely related to humans may be particularly promising.

The common marmoset (*Callithrix jacchus*) is classified into the Callitrichidae family of Platyrrini (New World monkeys) and has been used as a non-human primate experimental animal in various research fields including gene therapy, autoimmune disease, organ transplantation, and pharmacology (Kendall et al., 1998; Doods et al., 2000; Deisboeck et al., 2003; t'Hart et al., 2003). Accordingly, it is worth promoting studies with the common marmoset aimed at overcoming neurodegenerative diseases such as HD, as the animal's close relationship to humans makes it well suited to this kind of study. Indeed, a recent study has generated a non-human primate HD model with the rhesus monkey (*Macaca mulatta*) (Palfi et al., 2007; Yang et al., 2008).

In this report, we describe for the first time the isolation and characterization of a cDNA encoding the putative full-length open reading frame of the common marmoset *Htt* gene, and present experimental data based on the isolated cDNA. The data presented here may provide us with useful information for establishing non-human primate HD models with the common marmoset.

2. Materials and methods

2.1. Preparation of total RNA

Common marmoset total RNA was isolated from the brain tissue of a stillborn marmoset fetus and immortalized monocytes (described below) using Trizol (Invitrogen). The experiments with the common marmoset complied with protocols approved by the ethical committee for primate research of the National Center of Neurology and Psychiatry and adhered to the legal requirements of Japan.

Abbreviations: HD, Huntington's disease; Htt, huntingtn; RNAi, RNA interference; cDNA, complementary DNA; PBMC, peripheral blood mononuclear cell; RT, reverse transcription; PCR, polymerase chain reaction; ORF, open reading frame; APP, amyloid precursor protein; GAPDH, glyceraldehyde-3-phosphate dehydrogenase; GFP, green fluorescence protein; CMV, Cytomegalovirus.

* Corresponding author.
E-mail address: hohjohh@ncnp.go.jp (H. Hohjoh).

0378-1119/$ – see front matter © 2008 Elsevier B.V. All rights reserved.
doi:10.1016/j.gene.2008.11.012

2.2. Established common marmoset cell lines

Adult common marmosets being reared at the Primate Research Institute of Kyoto University or Tsukuba Primate Research Center were anesthetized by ketamine, which was approved by the Animal Welfare and Animal Care Committees of both institutes, and peripheral blood was collected. From the collected blood samples, peripheral blood mononuclear cells (PBMCs) were purified and immortalized by infection of a 488-77 strain of *Herpesvirus saimiri* (kindly provided by Dr. R. C. Desrosiers) as previously described (Akari et al., 1996). The established marmoset cell lines, designated HSCj-110, HSCj-009, and HSCj-002, were phenotypically activated CD3+T lymphocytic cells and grown in RPMI-1640 medium (Sigma) supplemented with 10% FCS, 50 mM 2-mercaptoethanol, and antibiotics.

2.3. Reverse transcription – (real time) polymerase chain reaction [RT-(real time) PCR]

The common marmoset total RNAs were subjected to complementary DNA (cDNA) synthesis using oligo(dT) primers and a Superscript III reverse transcriptase (Invitrogen), according to the manufacturer's instructions, and polymerase chain reaction (PCR) using the cDNAs as templates was carried out by means of the ABI GeneAmp PCR system 9700 (Applied Biosystems). In the case of real time PCR, the cDNAs were examined by the AB 7300 Real Time PCR System (Applied Biosystems) with a TaqMan Universal PCR Master Mix together with Assays-on-Demand Gene Expression products (Applied Biosystems) or a SYBR Green PCR Master Mix together with Perfect Real Time Primers (Takara Bio) or designed PCR primers, according to the manufacturers' instructions. Synthesized oligonucleotide primers and purchased primer and probe were as follows:

Synthesized oligonucleotide primers:

HD1-F: 5′-TATAGAATTCGGGAGACCGCCATGGCGAC-3′
HD1-ORF-R: 5′-TCAAGCGGCCGCTCAGCAGGTGGTGACCTTG-3′
HD1-1900R2: 5′-TAAAGGATCCCCGTCTAACACAATTTCAG-3′
cjHtt(1139)-F: 5′-TTATAGCTGGAGGCGGTTCC-3′
cjHtt(1254)-R: 5′-GACGTCCGACCTCGATTCAG-3′

Purchased primer and probe:

Assays-on-Demand Gene Expression product for the human *Htt* gene (Assay ID: Hs00169273_m1) (Applied Biosystems).

Perfect Real Time Primers for the human *GAPDH* gene (Primer-Set ID: HA067812) (Takara Bio).

2.4. Cloning and sequence analysis of the full-length ORF of the marmoset Htt gene

Complementary DNA derived from the common marmoset total RNA was subjected to PCR amplification using *TaKaRa LA Taq* polymerase (TAKARA BIO) with the HD1-F and HD1-ORF-R primers under the following thermal cycling conditions: heat denaturation at 94 °C for 1 min, 30 cycles of amplification including denaturation at 94 °C for 20 s and extension at 68 °C for 12 min, and a final extension at 72 °C for 10 min. The PCR product was examined by agarose gel electrophoresis followed by ethidium bromide staining, and an approximately 9.4 kb PCR band (Fig. 1) was purified from the gels using a TOPO XL gel purification kit (Invitrogen). The resultant PCR product was inserted into the pCR-XL-TOPO plasmid with a TOPO XL PCR cloning kit (Invitrogen) and then sequence determination of the insert was carried out. To clarify uncertain nucleotide sequences, additional RT-PCR targeting of uncertain regions followed by sequence determination was performed and the precise nucleotide sequence was confirmed. The determined nucleotide sequence encoding a putative full-length ORF of the common marmoset *Htt* gene has been registered in the GenBank database: accession number, AB443866.

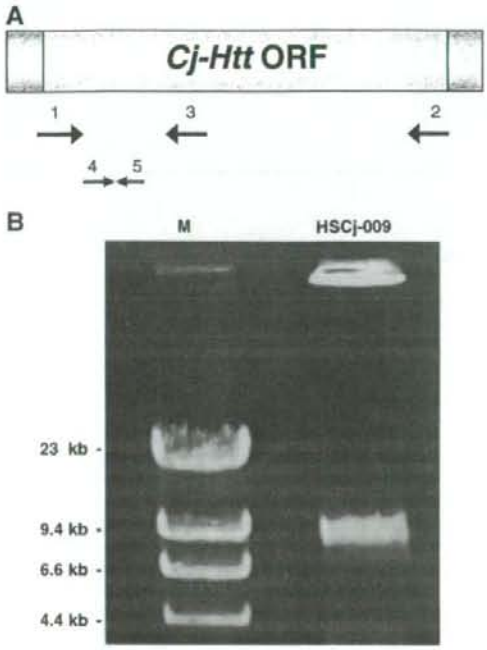

Fig. 1. RT-PCR amplification. (A) Schematic drawing of putative *Htt* cDNA. Open reading frame (ORF) is indicated by a yellow box. Arrows indicate synthesized PCR primers, which are designed in possibly conserved nucleotide sequences: 1, HD1-F; 2, HD1-ORF-R; 3, HD1-1900R2; 4, cjHtt(1139)-F; 5, cjHtt(1254)-R (detailed in Materials and methods). (B) RT-PCR. The first strand cDNA was synthesized by RT using RNA isolated from immortalized common marmoset mononuclear cells (HSCj-009) as a template and oligo(dT) as a primer. The following PCR was carried out using HD1-F and HD1-ORF-R primers. The resultant PCR products were analyzed by gel electrophoresis with 0.6 % agarose gel followed by ethidium bromide staining. Hind III-digested λDNA was used as a DNA size marker (M). (For interpretation of the references to colour in this figure legend, the reader is referred to the web version of this article.)

2.5. Western blotting

Equal amounts (~35 μg) of protein extracts from the common marmoset and mouse brain tissues and established PBMC lines (described above) were separated by SDS-PAGE with 5% polyacrylamide gels and electrophoretically blotted onto PVDF membranes (Millipore). Membranes were blocked for 1 h in blocking solution [5% non-fat milk in TBST buffer (25 mM Tris-HCl, pH 7.4, 150 mM NaCl and 0.1% Tween-20)] and incubated with 1/1000 dilution of mouse anti-huntingtin protein monoclonal antibodies [MAB2166 and MAB2170 (Chemicon); ab7666 (Abcam)] followed by washing in TBST buffer and further incubation with sheep anti-mouse Ig, HRP-linked whole Ab (GE Healthcare). Antigen-antibody complexes were visualized using ECL plus Western Blotting Detection Reagent (GE Healthcare). After detection of signals, the membranes were subjected to antibody removal in Re-Blot Plus strong antibody stripping solution (Chemicon) followed by washing in TBST buffer, and then incubated with 1/1000 dilution of mouse anti-APP [MAB348 (Chemicon)] monoclonal antibody. Subsequent processes were the same as described above.

2.6. Gene silencing of marmoset Htt by RNA interference

To monitor gene silencing against the common marmoset *Htt* gene, we constructed a reporter plasmid carrying the 5′-terminal region of the marmoset *Htt* linked with the *GFP* reporter gene: the PCR product obtained from RT-PCR with the HD1-F and HD1-1900R2 primers was

Table 1
Sequence homologies (%) among various species' *Htt* genes

Homo sapiens	*Callithrix jacchus*	*Canis lupus familiaris*	*Bos taurus*	*Sus scrofa*	*Mus musculus*	*Rattus norvegicus*
Homo sapiens	**95.1** **97.0**	87.0 92.0	84.0 89.5	84.1 88.6	86.1 91.2	85.8 91.2
Canis lupus familiaris		86.6 91.4	84.0 88.4	83.9 87.9	85.6 90.8	85.1 90.9
Callithrix jacchus			84.5 89.4	84.4 89.7	84.0 89.2	83.8 89.3
Bos taurus				86.8 89.3	81.2 87.1	81.3 87.4
Sus scrofa					80.9 86.9	80.8 87.2
Mus musculus						95.9 97.6
Rattus norvegicus						

Figures in upper and lower stands represent nucleotide and amino acid sequence homologies, respectively, between two species.

trimmed with EcoRI and BamHI, and inserted into the pd2EGFP-N1 plasmid (Clontech) treated with the same restriction enzymes. The resultant reporter (5′*Cj-Htt-GFP*) plasmid and synthetic siRNA duplex targeting the marmoset *Htt* (cjHtt-1 siRNA duplex) were cotransfected into mouse neuroblastoma Neuro2a cells by Lipofectamine 2000 transfection reagent (Invitrogen) as described previously (Sakai and Hohjoh, 2006). Two days after transfection, the cells were examined by a fluorescent microscope. When the endogenous marmoset *Htt* gene was inhibited by RNAi, the cjHtt-1 siRNA duplex (0.4 nmol/transfection) was introduced into HSCj-009 cells (1×10^6 cells/transfection) by means of a Nucleofector system (Amaxa Biosystems) according to the manufacturer's instructions. Two days after transfection, total RNA and cell lysate were prepared from the cells and examined by RT-real time PCR and Western blotting, respectively.

The nucleotide sequences of synthesized cjHtt-1 siRNA were as follows:

Sense: 5′-GCCUUUGAGUCCCUCAAGUUU-3′
Antisense: 5′-ACUUGAGGGACUCAAAGGCUU-3′

2.7. Sequence data and computational analyses

The *Htt* sequnece data derived from various species were as follows [GenBank accession number]: human (*Homo sapiens*) [NM_002111]; chimp (*Pan troglodytes*) [XM_517080]; rhesus macaque (*Macaca mulatta*) [XM_001086119]; canine (*Canis lupus familiaris*) [XM_536221]; bovine (*Bos taurus*) [XM_866758]; wild boar (*Sus scrofa*) [NM_213964]; mouse (*Mus musculus*) [NM_010414]; rat (*Rattus norvegicus*) [XM_573634]; chicken (*Gallus gallus*) [XM_420822]. Although the rhesus macaque Htt sequence [XM_001086119] contains 20 undetermined nuclotides at positons 4932–4951 followed by 6 suspensive amino acid sequences, the sequence was used and examined together with the other sequneces in this study.

Sequence homology analysis of either nucleotide or amino acid sequences was carried out by means of the GENETYX software (Software Development Co., Ltd., Tokyo, Japan), where all the parameters were set at default. For identification of the HEAT repeats in the Cj-Htt protein sequences, the REP program (http://www.embl-heidelberg.de/~andrade/papers/rep/search.html) developed by Andrade et al. was used.

3. Results and discussion

3.1. Isolation and characterization of the common marmoset Htt gene

To isolate and identify the common marmoset *Htt* (*Cj-Htt*) gene and/or gene products, we focused on conserved regions in the *Htt* gene and isolate cDNA clone of the *Cj-Htt* transcript. Highly homologous regions (sequences) between the human and mouse *Htt* genes, whose corresponding regions in the *Cj-Htt* gene were also expected to remain conserved, were selected, and PCR primers were designed for such regions. We add that such conserved regions are also detectable by BLAST search with the human *Htt* as a query on the Trace archive of the Cj-database in NCBI. RT-PCR with the designed primers and total RNA extracted from common marmoset brain tissue and established cell lines was carried out, and an approximately 9.4 kb long PCR product, which was expected to contain the full-length open reading frame (ORF) of *Cj-Htt*, was obtained (Fig. 1). The PCR product was subjected to sequence determination and then compared with various species' *Htt* genes. From the results, it was clear that the PCR product, which is 9396 nucleotides in length, was derived from the common marmoset *Htt* gene which encodes a predicted 3131 amino acid long Cj-Htt polypeptide (the sequence accession number in GenBank is AB443866). Sequence homologies in the *Htt* gene among various species are indicated in Table 1. From the data, it appears that both the nucleotide and predicted amino acid sequences of the *Cj-Htt*

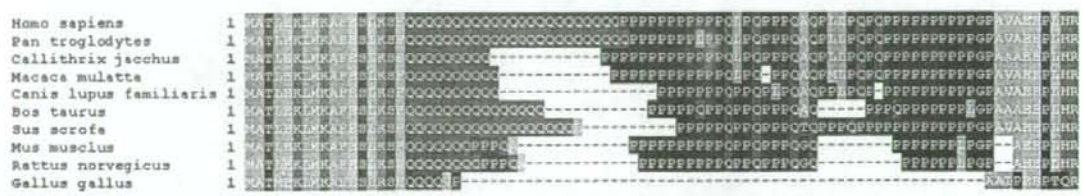

Fig. 2. Alignment of amino acid sequences in the Htt exon 1 and its corresponding regions. Sequence data were aligned based on the human Htt exon 1 (top line). Amino acid residues are color-coded based on the biochemical properties of the residues: hydrophobic amino acids in orange, polar amino acids with uncharged R groups in green, acidic amino acids in pink, basic amino acids in light blue, and special amino acids in dark blue.

Table 2
Alignment of HEAT repeats

Repeat*	Species**	AA position		Fragment†	Score	E-value
		From	To			
HEAT_AAA	Hs - Htt	124	162	QKLLGIAMELFLLCSDDAESDVRMVADECLNKVIKALMD	1510	1.26E-06
	Cj - Htt	112	150	QKLLGIAMELLLLCSDDAESDVRMVADECLNKVIKALMD	1590	5.48E-07
HEAT_AAA	Hs - Htt	205	243	RPYLVNLLPCLTRTSKRPEESVQETLAAAVPKIMASFGN	1990	1.03E-04
	Cj - Htt	193	231	RPYLVNLLPCLTRTSKRPEESVQETLAAAVPKIMASFGN	1990	2.37E-08
HEAT_AAA	Hs - Htt	247	285	DNEIKVLLKAFIANLKSSSPTIRRTAAGSAVSICQHSRR	1590	5.48E-07
	Cj - Htt	235	273	DNEIKLLLKAFIANLKSSSPTIRRTAAGSAVSICQHSRR	1590	1.97E-06
HEAT_AAA	Hs - Htt	317	355	LLTLRYLVPLLQQQVKDTSLKGSFGVTRKEMEVSPSAEQ	1620	1.11E-06
	Cj - Htt	305	343	LLTLRYLVPLLHQQVKDTSLKGSFGVTRKEMEVSPSAEQ	1570	1.46E-07
HEAT_ADB	Hs - Htt					
	Cj - Htt	734	771	YPEEQYVSDILNYIDHGDPQVRGATAILCGTLVCSILS	1450	3.29E-07
HEAT_AAA	Hs - Htt	803	841	TFSLADCIPLLRKTLKDESSVTCKLACTAVRNCVMSLCS	1500	5.78E-07
	Cj - Htt	791	829	TFSLADCVPLLRKTLKDESSVTCKLACTAVRHCVMSLCS	1449	2.90E-06
HEAT_AAA	Hs - Htt	904	942	KLQERVLNNVVIHLLGDEDPRVRHVAAASLIRLVPKLFY	1930	6.69E-08
	Cj - Htt	892	930	TLQERVLTSVVIHLLGDEDPRVRHVAAASLIRLVPKLFY	2150	2.51E-05
HEAT_AAA	Hs - Htt	984	1025	RIYRGYNLLPSITDVTMENNLSRVIAAVSHELITSTTRALTF	1370	9.05E-06
	Cj - Htt	972	1013	RIYRGYNLLPSIIDVTMENNLSRVIAAVSHELITSTTRALTF	1410	2.71E-06
HEAT_AAA	Hs - Htt	1425	1463	RLFEPLVIKALKQYTTTTCVQLQKQVLDLLAQLVQLRVN	1370	5.62E-06
	Cj - Htt	1413	1451	RLFEPLVIKALKQYTTTTSVQLQKQVLDLLAQLVQLRVN	1580	3.20E-07
HEAT_AAA	Hs - Htt	2798	2836	DDTAKQLIPVISDYLLSNLKGIAHCVNIHSQQHVLVMCA	1430	3.51E-06
	Cj - Htt	2785	2823	DDTAKQLIPVISDYLLSSLKGLAHCVNTHSQQHVLVMCA	1430	3.29E-06

* HEAT_AAA and HEAT_ADB indicate subsets of HEAT repeats representing PP2A and adaptin families, respectively.
** Hs-Htt and Cj-Htt indicate the human and common marmoset Htt proteins, respectively.
†Amino acids which are different from the sequence of Hs-Htt are indicated in red.

cDNA have significant sequence homology to that of other species' *Htt* genes. In addition, it should be noted that *Htt* sequences between the human and common marmoset (colored in yellow in Table 1) appear to be particularly conserved as compared with sequence conservation within non-primate *Htt* genes, suggesting that the *Htt* gene is highly conserved in primates.

Fig. 2 shows the alignment of amino acid sequences encoded by *Htt* exon 1 and its corresponding region in various species. From the alignment, *Cj-Htt* appears to possess a short polyglutamine tract of nine glutamines compared with that of the human and chimpanzee *Htt* genes; but other than the polyglutamine tract, the exon 1 corresponding region in *Cj-Htt* exhibits high sequence homology to the human *Htt* exon 1. It is also interesting that polyproline region adjacent to the polyglutamine tract has differences between primates and non-primates: amino acid substitutions and deletions are observed, and the lack of the polyproline region in the *Gallus gallus Htt* exon 1 is particularly remarkable. These differences may influence folding and aggregation of the Htt protein, and might represent adaptive evolution of *Htt* to each species. The difference in the exon 1 among various species may provide us with a hint for understanding the expansion of the polyglutamine tract in Huntington's disease in human.

Other than the exon 1 region, we also investigated the HEAT repeats possessing tandem arrayed bihelical structure, which appear to wrap around target substrates (Andrade and Bork, 1995; Neuwald and Hirano, 2000), and found that the HEAT repeats are also conserved in the Cj-Htt protein (Table 2). In addition, it may be interesting that HEAT_ADB, a subset of HEAT repeats representing adaptin family, is present in Cj-Htt, but not in Hs-Htt.

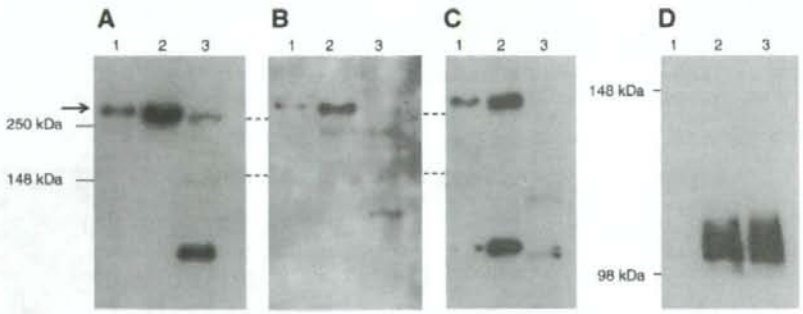

Fig. 3. Assessment of anti-human Htt antibodies against the common marmoset Htt polypeptide. Cell lysate derived from the common marmoset cell line (HSCj-110) (lane 1), brain tissue (lane 2), and mouse brain tissue as a control (lane 3) was examined by Western blotting with anti-human Htt antibodies. Tested antibodies were as follows: (A) MAB2166 (Chemicon), (B) MAB2170 (Chemicon), and (C) ab7666 (Abcam). Arrow indicates the signals of Htt proteins. The same results as those of HSCj-110 were also obtained when HSCj-002 and-009 were used (data not shown). After detection of signals, blotted membranes were subjected to antibody removal and then incubated with anti-APP antibody [MAB348 (Chemicon)] (D) followed by the same procedure as in the anti-human Htt antibodies described above.

3.2. Detection of *Cj-Htt* gene products

It is important to be able to properly detect the *Cj-Htt* gene and its gene products. Since the nucleotide and predicted amino acid sequences of the *Cj-Htt* cDNA showed significantly high sequence homologies to those of the human *Htt* gene, we tested whether commercially-available TaqMan probe and antibodies against human *Htt* gene products (mRNA and protein) were also able to detect *Cj-Htt* gene products. As a result, the TaqMan probe (Fig. 5A) appears to be able to detect *Cj-Htt* mRNA. In addition, newly designed PCR primers, which are perfectly matched to *Cj-Htt*, also appear to be able to detect *Cj-Htt* mRNA (Fig. 5B).

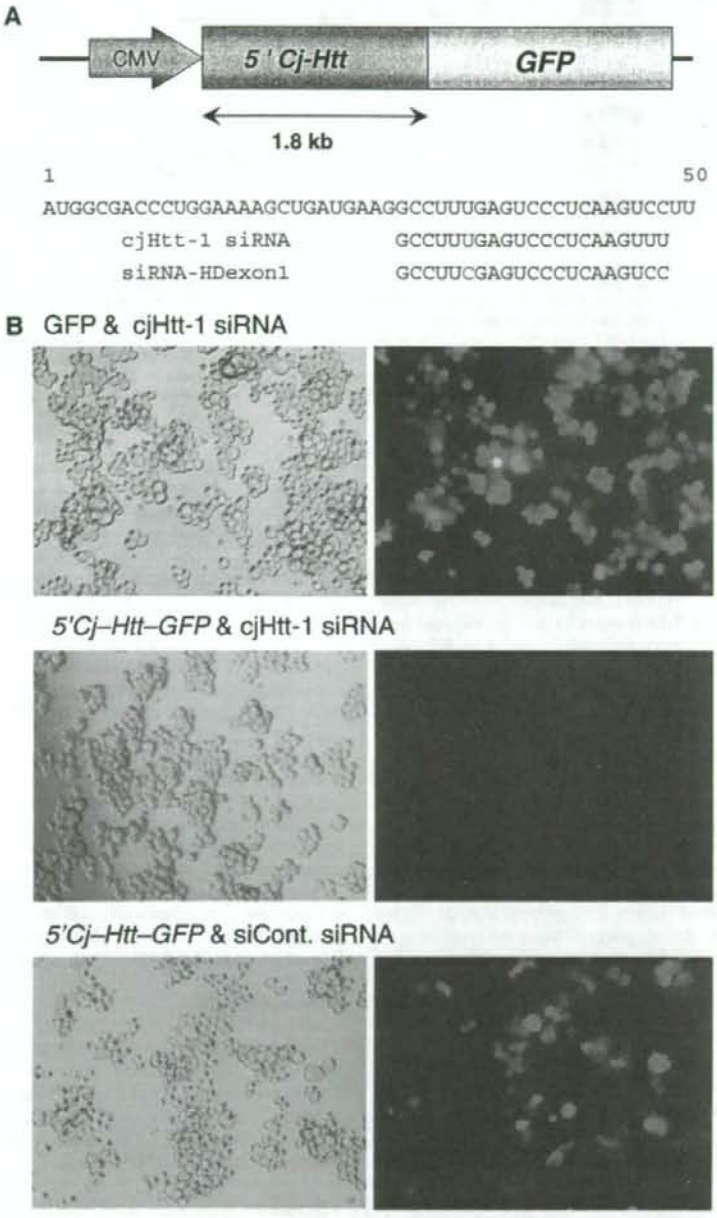

Fig. 4. Gene silencing against the 5′*Cj-Htt-GFP* fusion gene. (A) Schematic drawing of the 5′*Cj-Htt-GFP* fusion gene and designed cjHtt-1 siRNA. The fusion gene is composed of the 5′ terminal region of the Cj-Htt ORF and GFP, and driven by the Human cytomegalovirus promoter. The *Cj-Htt* sequence from the first ATG to position 50 is shown together with sequences of cjHtt-1 siRNA and siRNA-HDexon1 targeting human *Htt*. A variant nucleotide between the siRNAs is indicated in red. (B) Effect of cjHtt-1 siRNA on gene silencing. Reporter genes [5′*Cj-Htt-GFP* or *GFP* (empty reporter)] and siRNAs [cjHtt-1 or siCont (non-silencing siRNA)] were introduced into mouse neuroblastoma Neuro2a (N2a) cells. Two days after transfection, the cells were examined by a fluorescent microscope. Left (differential interference contrast) and right (fluorescence image) panels are identical in the visual field.

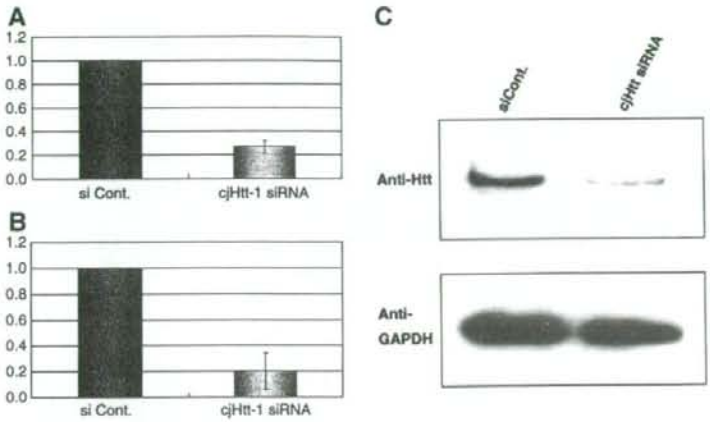

Fig. 5. Inhibition of expression of endogenous *Cj-Htt* by RNAi. The cjHtt-1 siRNA was introduced into HSCJ-009 cells by means of electroporation. Two days after transfection, total RNA and cell lysate were prepared and examined by RT-real time PCR and Western blotting, respectively. Total RNA was subjected to cDNA synthesis as in Fig. 1. The resultant cDNA was examined by real time PCR with a TaqMan probe for the human *Htt* gene (A) and newly designed PCR primers [cjHtt(1139)-F and cjHtt(1254)-R] (B). The expression of *Gapdh* as a control was also examined using Perfect Real Time Primers for the human *GAPDH* gene (TAKARA BIO). The expression level of *Cj-Htt* was normalized against that of *Gapdh*, and the ratios of *Cj-Htt* expression level in the presence of cjHtt-1 siRNA were normalized against the ratio obtained in the presence of the siControl siRNA (siCont.). Data are means of at least three independent determinations. Error bars represent standard deviations. (C) Western blot. Cell lysate was examined by Western blotting with anti-human Htt antibody (MAB2166; Chemicon) as in Fig. 3. After detection of signals, the expression of GAPDH as a control was also examined by anti-GAPDH antibody (AM4300; Ambion).

Western blot analyses indicate that a polypeptide of approximately 350 kDa, which is almost the same as the molecular weight estimated from the amino acid sequence (346 kDa) in the *Cj-Htt* cDNA, can be detected in the common marmoset specimens by the antibodies tested, suggesting that the Cj-Htt protein is detectable with the antibodies (Figs. 3A–C). The 350 kDa mouse Htt protein was detected by the MAB2166 antibody (Fig. 3A), but hardly with the other antibodies (Figs. 3B and C). This may be caused by possibly low expression level of mouse Htt in the brain tissue, and/or by difference in the epitope sequences between the common marmoset and mouse Htt proteins. Other than the 350 kDa band, a few bands migrated faster than the 350 kDa band were also observed. They may be degradation products of the Htt protein, and different cells and/or species might have different degradation of the protein. To clarify these, further studies need to be carried out.

In addition to the Htt protein, we also examined the expression of amyloid precursor protein (App) with the 22C11 antibody, which can recognize the same amino acid sequence at positions 66–81 of either the human or mouse App. As a result, the App signal was able to be detected in either the common marmoset or mouse brain tissue, but not in the common marmoset immortalized peripheral blood mononuclear cells (PBMCs) (Fig. 3D), suggesting little or no expression of App in PBMCs and availability of the antibody for detection of the Cj-App protein.

3.3. Gene silencing against the Cj-Htt gene

To verify the data presented here and tools for the detection of *Cj-Htt*, we carried out gene silencing against the expression of endogenous *Cj-Htt* by means of RNA interference (RNAi), and assessed the knockdown potency of designed siRNA targeting *Cj-Htt* using the tools evaluated above. Based on a previous study where a competent siRNA duplex, siRNA-HDexon 1, conferring strong inhibition against the expression of the human *Htt* gene was used (Liu et al., 2003), we chemically synthesized an siRNA duplex, cjHtt-1 siRNA, corresponding to the siRNA-HDexon 1 duplex; note that there is one nucleotide change between cjHtt-1 siRNA and siRNA-HDexon 1 (Fig. 4A).

To examine the effect of the siRNA duplex on gene silencing, we constructed a reporter plasmid carrying the 5′ terminal region of *Cj-Htt* cDNA linked with the *GFP* reporter gene (the 5′*Cj-Htt-GFP* fusion gene). The reporter plasmid and the siRNA were cotransfected into mouse Neuro2a cells, and the expression of the 5′*Cj-Htt-GFP* fusion gene was examined by a fluorescent microscope. As shown in Fig. 4B, the data indicated that the cjHtt-1 siRNA duplex was able to induce strong RNAi activity against the fusion gene expression.

Next, we introduced the cjHtt-1 siRNA duplex into immortalized common marmoset mononuclear cells by means of electroporation, and two days after transfection, the expression levels of the endogenous *Cj-Htt* mRNA and protein were examined by RT-real time PCR and Western blotting, respectively. As shown in Fig. 5, the results consistently indicated that *Cj-Htt* mRNA (A and B) and protein (C) levels markedly decreased in the presence of the cjHtt-1 siRNA duplex, i.e., potent RNAi knockdown against the endogenous *Cj-Htt* gene was induced by the siRNA duplex. Finally, the data presented here also indicate that proper detection of the newly identified *Cj-Htt* gene and its products can be performed by means of the methods and tools assessed in this study.

In conclusion, we described for the first time the common marmoset *Htt* gene, and also detection methods and tools for the gene and its gene products. The data presented here may assist us in promoting a non-human primate HD model with the common marmoset.

Acknowledgments

We would like to thank Dr. R.C. Desrosiers for kindly providing HS viruses. We also thank Drs. K. Nakamura, T. Kabuta, M. Suzuki, and C. Konya for their helpful advice and discussion. Finally, we would like to thank Dr I. Kanazawa for his encouragement and helpful advice. This work was supported by research grants from the Ministry of Health, Labour and Welfare of Japan.

References

Akari, H., et al., 1996. In vitro immortalization of Old World monkey T lymphocytes with Herpesvirus saimiri: its susceptibility to infection with simian immunodeficiency viruses. Virology 218, 382–388.

Andrade, M.A., Bork, P., 1995. HEAT repeats in the Huntington's disease protein. Nat. Genet. 11, 115–116.

Deisboeck, T.S., et al., 2003. Development of a novel non-human primate model for preclinical gene vector safety studies. Determining the effects of intracerebral HSV-1 inoculation in the common marmoset: a comparative study. Gene Ther. 10, 1225–1233.
Doods, H., et al., 2000. Pharmacological profile of BIBN4096BS, the first selective small molecule CGRP antagonist. Br. J. Pharmacol. 129, 420–423.
Gilliam, T.C., et al., 1987. A DNA segment encoding two genes very tightly linked to Huntington's disease. Science 238, 950–952.
Gusella, J.F., et al., 1983. A polymorphic DNA marker genetically linked to Huntington's disease. Nature 306, 234–238.
Huntington's-Disease, C.R.G.o., The Huntington's Disease Collaborative Research Group, 1993. A novel gene containing a trinucleotide repeat that is expanded and unstable on Huntington's disease chromosomes. Cell 72, 971–983.
Kazemi-Esfarjani, P., Benzer, S., 2000. Genetic suppression of polyglutamine toxicity in Drosophila. Science 287, 1837–1840.
Kendall, A.L., Rayment, F.D., Torres, E.M., Baker, H.F., Ridley, R.M., Dunnett, S.B., 1998. Functional integration of striatal allografts in a primate model of Huntington's disease. Nat. Med. 4, 727–729.
Liu, W., Goto, J., Wang, Y., Murata, M., Wada, K., Kanazawa, I., 2003. Specific inhibition of Huntington's disease gene expression by siRNAs in cultured cells. Proc. Jpn. Acad. 79, 293–298.
Lunkes, A., Mandel, J.L., 1998. A cellular model that recapitulates major pathogenic steps of Huntington's disease. Hum. Mol. Genet. 7, 1355–1361.
Mangiarini, L., et al., 1996. Exon 1 of the HD gene with an expanded CAG repeat is sufficient to cause a progressive neurological phenotype in transgenic mice. Cell 87, 493–506.
Neuwald, A.F., Hirano, T., 2000. HEAT repeats associated with condensins, cohesins, and other complexes involved in chromosome-related functions. Genome Res. 10, 1445–1452.
Palfi, S., et al., 2007. Expression of mutated huntingtin fragment in the putamen is sufficient to produce abnormal movement in non-human primates. Mol. Ther. 15, 1444–1451.
Sakai, T., Hohjoh, H., 2006. Gene silencing analyses against amyloid precursor protein (APP) gene family by RNA interference. Cell Biol. Int. 30, 952–956.
t'Hart, B.A., Vervoordeldonk, M., Heeney, J.L., Tak, P.P., 2003. Gene therapy in nonhuman primate models of human autoimmune disease. Gene Ther. 10, 890–901.
von Horsten, S., et al., 2003. Transgenic rat model of Huntington's disease. Hum. Mol. Genet. 12, 617–624.
Walker, F.O., 2007. Huntington's disease. Lancet 369, 218–228.
Yang, S.H., et al., 2008. Towards a transgenic model of Huntington's disease in a non-human primate. Nature 453, 921–924.

OPEN ACCESS Freely available online

PLoS one

Enhancement of Allele Discrimination by Introduction of Nucleotide Mismatches into siRNA in Allele-Specific Gene Silencing by RNAi

Yusuke Ohnishi[1,2], Yoshiko Tamura[1], Mariko Yoshida[1], Katsushi Tokunaga[2], Hirohiko Hohjoh[1]*

1 Department of Molecular Genetics, National Institute of Neuroscience, NCNP, Kodaira, Tokyo, Japan, 2 Department of Human Genetics, Graduate School of Medicine, The University of Tokyo, Tokyo, Japan

Abstract

Allele-specific gene silencing by RNA interference (RNAi) is therapeutically useful for specifically inhibiting the expression of disease-associated alleles without suppressing the expression of corresponding wild-type alleles. To realize such allele-specific RNAi (ASP-RNAi), the design and assessment of small interfering RNA (siRNA) duplexes conferring ASP-RNAi is vital; however, it is also difficult. In a previous study, we developed an assay system to assess ASP-RNAi with mutant and wild-type reporter alleles encoding the *Photinus* and *Renilla luciferase* genes. In line with experiments using the system, we realized that it is necessary and important to enhance allele discrimination between mutant and corresponding wild-type alleles. Here, we describe the improvement of ASP-RNAi against mutant alleles carrying single nucleotide variations by introducing base substitutions into siRNA sequences where original variations are present in the central position. Artificially mismatched siRNAs or short-hairpin RNAs (shRNAs) against mutant alleles of the human *Prion Protein* (*PRNP*) gene, which appear to be associated with susceptibility to prion diseases, were examined using this assessment system. The data indicates that introduction of a one-base mismatch into the siRNAs and shRNAs was able to enhance discrimination between the mutant and wild-type alleles. Interestingly, the introduced mismatches that conferred marked improvement in ASP-RNAi appeared to be largely present in the guide siRNA elements, corresponding to the 'seed region' of microRNAs. Due to the essential role of the 'seed region' of microRNAs in their association with target RNAs, it is conceivable that disruption of the base-pairing interactions in the corresponding seed region, as well as the central position (involved in cleavage of target RNAs), of guide siRNA elements could influence allele discrimination. In addition, we also suggest that nucleotide mismatches at the 3'-ends of sense-strand siRNA elements, which possibly increase the assembly of antisense-strand (guide) siRNAs into RNA-induced silencing complexes (RISCs), may enhance ASP-RNAi in the case of inert siRNA duplexes. Therefore, the data presented here suggest that structural modification of functional portions of an siRNA duplex by base substitution could greatly influence allele discrimination and gene silencing, thereby contributing to enhancement of ASP-RNAi.

Citation: Ohnishi Y, Tamura Y, Yoshida M, Tokunaga K, Hohjoh H (2008) Enhancement of Allele Discrimination by Introduction of Nucleotide Mismatches into siRNA in Allele-Specific Gene Silencing by RNAi. PLoS ONE 3(5): e2248. doi:10.1371/journal.pone.0002248

Editor: Luis M. Corrochano, University of Sevilla, Spain

Received November 1, 2007; **Accepted** April 14, 2008; **Published** May 21, 2008

Funding: This work was supported in part by research grants from the Ministry of Health, Labor, Welfare in Japan, and from Research Fellowships of the Japan Society for the Promotion of Science for Young Scientists, and also by a Grant-in-Aid from the Japan Society for the Promotion of Science.

Competing Interests: The corresponding author has a pending patent on the method used in this study.

* E-mail: hohjohh@ncnp.go.jp

Introduction

RNA interference (RNAi) is the process of sequence-specific posttranscriptional gene silencing induced by double-stranded RNAs (dsRNAs) homologous to the silenced gene, and it is currently used as a powerful tool to suppress the expression of genes of interest [1,2]. Introduced or generated dsRNAs are subjected to digestion by an RNase III enzyme, Dicer, into 21–25 nucleotide (nt) RNA duplexes [3]. The resultant RNA duplexes, referred to as small interfering RNA (siRNA) duplexes, are unwound, and single-stranded siRNA elements can then be incorporated into RNA-induced silencing complexes (RISCs) to function as sequence-specific mediators. These are referred to as guide siRNA elements [1,2,4].

In mammals, RNAi can be induced by direct introduction of chemically synthesized siRNA duplexes into cells, or by generation of siRNA duplexes using short-hairpin RNA (shRNA) expression vectors. Applications are expanding in various fields of science, with the potential therapeutic use of RNAi in medical science and pharmacogenesis being particularly promising [1,5–8].

Allele-specific gene silencing by RNAi (allele-specific RNAi: ASP-RNAi) is an advanced application of RNAi techniques that allows the expression of an allele of interest to be specifically inhibited [9]. ASP-RNAi would thus be therapeutically very useful, as it can specifically suppress the expression of alleles causing disease without inhibiting the expression of corresponding wild-type alleles [10–17]. To induce such ASP-RNAi, it is necessary to design siRNAs that exhibit strong allele-specific gene silencing; thus, siRNAs must be designed such that they are able to carry nucleotide variations characterizing target disease alleles and to discriminate the target alleles from corresponding wild-type alleles. In addition, qualitative and quantitative evaluation of such designed siRNAs on allele-specific gene silencing is required.

In a previous study, we developed an assay system to assess ASP-RNAi with mutant and wild-type reporter alleles encoding

the *Photinus* and *Renilla luciferase* genes. In this system, the effects of designed siRNAs and short-hairpin RNAs (shRNAs) against mutant alleles in allele-specific gene silencing, as well as off-target silencing against wild-type alleles, can be simultaneously examined [17]. With amyloid precursor protein (*APP*) variants (the Swedish- and London-type variants) related to familial Alzheimer's disease [18,19] as model disease alleles, we were able to determine competent siRNA duplexes conferring ASP-RNAi [17]. Previous observations have also suggested that enhanced discrimination of target mutant alleles carrying single nucleotide variations from wild-type allele RNAs is required for ASP-RNAi.

In the present study, we describe the improvement of ASP-RNAi against mutant alleles carrying single nucleotide variations. We introduced base substitutions into siRNA and shRNA sequences, and examined the effects of the resultant mismatched siRNAs and shRNAs on ASP-RNAi by means of our assay system. The results presented here suggest that base substitutions introduced into certain portions of siRNA and shRNA sequences may contribute to enhancement of ASP-RNAi.

Results

ASP-RNAi against *PRNP* alleles carrying single nucleotide variations

In a previous study, we established an assessment system for siRNA duplexes conferring ASP-RNAi [17]. This system depends on two reporter alleles encoding the *Photinus* and *Renilla luciferase* genes carrying mutant and wild-type allelic sequences in their 3′-UTRs. Briefly, using this system, the effects of test siRNA duplexes against mutant alleles in allele-specific silencing, as well as off-target silencing against wild-type alleles, can be examined under heterozygous conditions generated by cotransfecting the reporter alleles and siRNA duplexes into cultured human cells.

In this study, we focused on the human *Prion Protein (PRNP)* gene, which is known to possess a number of single nucleotide variations [20,21]. We selected three *PRNP* variants, which are also followed by amino acid substitutions (*P102L*, *P105L*, and *D178N*) and appear to be associated with susceptibility to various prion diseases such as Gerstmann-Sträussler-Scheinker disease (GSS) and fatal familial insomnia (FFI) [22–25]. We constructed three mutant reporter alleles, designated the *PRNP-P102L*, *PRNP-P105L*, and *PRNP-D178N* alleles, and their corresponding wild-type reporter alleles (Figure 1A). The reporter alleles, synthetic siRNA duplexes against the mutant alleles (supplementary Table s1 and supplementary Figure s1), and the *beta-galactosidase* gene (control), were cotransfected into HeLa cells; thus, the transfected cells were artificially heterozygous with the mutant and wild-type reporter alleles. The effects of the designed siRNA duplexes on suppression of both the mutant and wild-type alleles were then simultaneously examined. As shown in Figure 1, the siRNA duplexes other than siPrnp102(T7), siPrnp102(T8), siPrnp105(T7) and siPrnp105(T9) were not able to induce significant ASP-RNAi. Of the four siRNAs just listed, the siPrnp105(T9) duplex appears to confer ASP-RNAi.

To realize ASP-RNAi against any target alleles, it is important and necessary to establish techniques for enhancement of allele discrimination followed by specific digestion against the target alleles. To address this, we selected siRNA duplexes possessing strong knockdown potency as candidates for improvement. This is because the only apparent failure of such siRNAs is being unable to discriminate target alleles from non-target ones, i.e., ASP-RNAi may be improved just by reinforcing allele discrimination. Since RNAi activity appears to be influenced by nucleotide mismatches

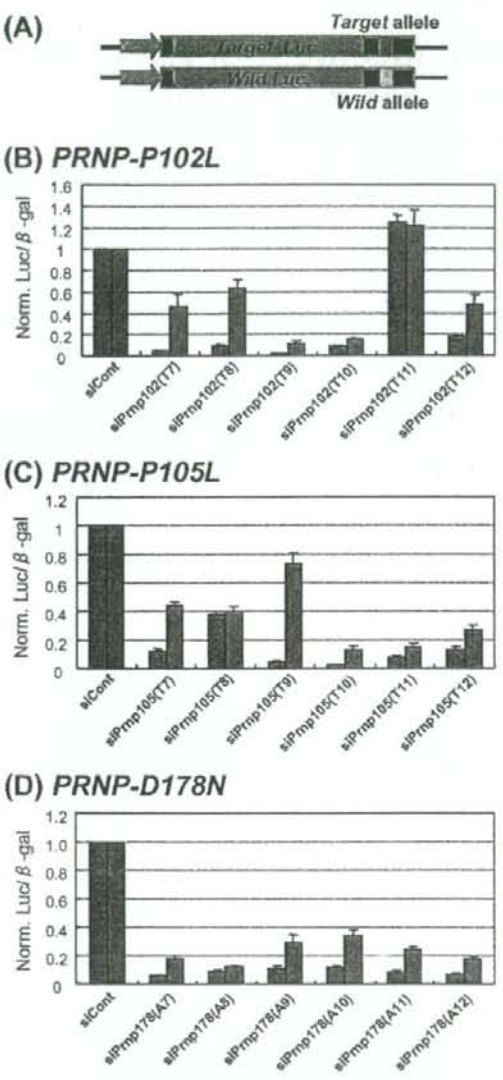

Figure 1. Assessment of ASP-RNAi with reporter alleles. (A) Schematic drawing of reporter alleles. Reporter alleles were constructed by inserting synthetic oligonucleotides of mutant and wild-type allelic sequences into the 3′-UTRs of the reporter genes driven by the same TK promoter (indicated by arrows). Assessment of designed siRNA duplexes against the mutant allele was carried out as described in Materials and Methods. Effects of designed siRNA duplexes against the *PRNP-P102L* (B), *PRNP -P105L* (C), and *PRNP -D178N* (D) mutants on ASP-RNAi. Reporter alleles, synthetic siRNA duplexes against the mutant alleles (indicated) and the *β-galactosidase* gene (control) were cotransfected into HeLa cells. Twenty-four hours after transfection, expression levels of the reporter genes were examined. Levels of either mutant allele (pink boxes) or wild-type allele (blue boxes) luciferase activity were normalized against the levels of β-galactosidase activity, and the ratios of mutant and wild-type luciferase activities in the presence of siRNA duplexes were normalized against the control ratios obtained in the presence of siControl duplex (siCont). Data are averages of at least three independent determinations. Error bars represent standard deviations.
doi:10.1371/journal.pone.0002248.g001

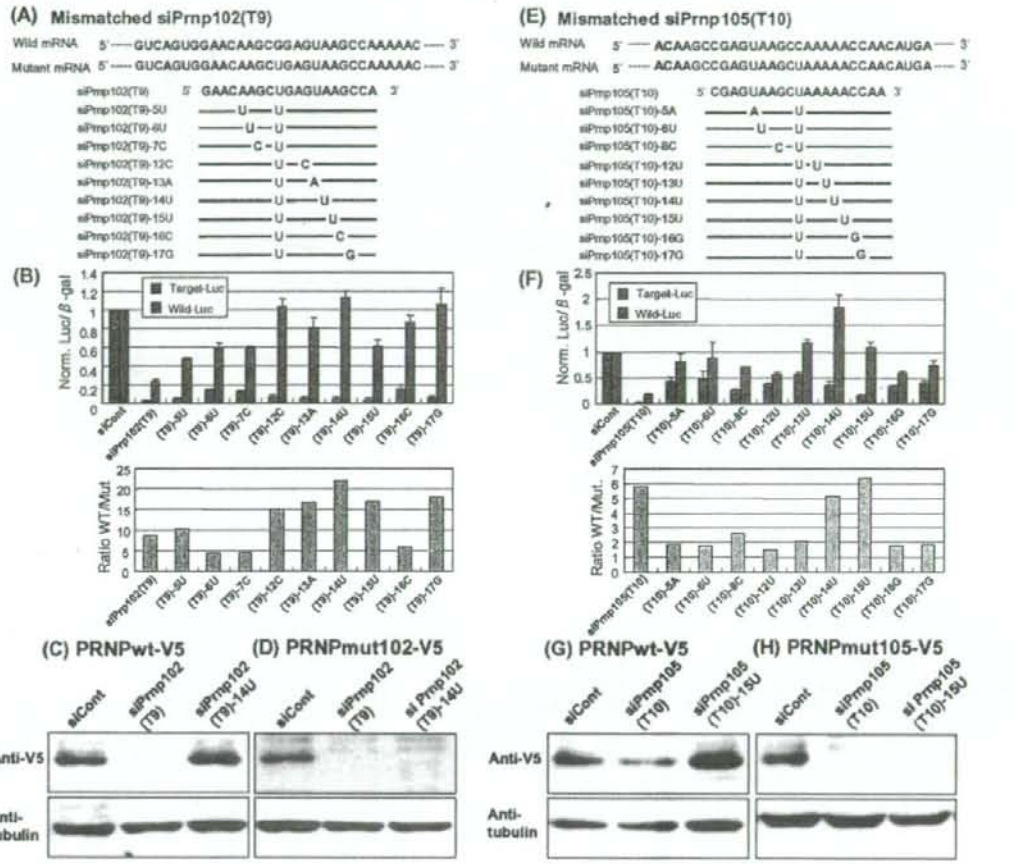

Figure 2. Assessment of mismatched siPrnp102(T9) and siPrnp105(T10) duplexes on ASP-RNAi. (A, E) Nucleotide sequences of wild-type and mutant *PRNP* mRNAs and designed siRNAs. The wild-type and mutant *PRNP* mRNA sequences around the P102L (A) and P105L (E) variations are shown and the variations are indicated in red. Designed siRNAs (indicated) are represented based on the sequence of the sense-strand (passenger) siRNA element; mismatched nucleotides (introduced base substitutions) and the original variations are indicated in blue and red, respectively. The same sequences as the siPrnp102(T9) or siPrnp105(T10) are represented by thin lines. (B, F) Effects of mismatched siPrnp102(T9) and siPrnp105(T10) on ASP-RNAi. Mismatched siPrnp102(T9) (B) and siPrnp105(T10) (E) duplexes (indicated) were examined as in Figure 1. The ratio of wild-type allele-luciferase activity against the mutant allele-luciferase activity (WT/Mut) was also examined to evaluate the improvement in ASP-RNAi. Data are averages of at least three independent determinations. Error bars represent standard deviations. Expression of the wild-type (C, G) and mutant [P102L (D) and P105L (H)] PRNP polypeptides (PRNPmut102-V5 and PRNPmut102-V5) in the presence of indicated siRNA duplexes was investigated by Western blotting using anti-V5 antibody. Expression of α-tubulin was examined as the control.
doi:10.1371/journal.pone.0002248.g002

between siRNAs and their target RNAs [11,26], we introduced a one-base substitution into the selected siRNAs (Figures 2A and E; supplementary Table s2) and examined the effects of such mismatched siRNA duplexes using our assessment system. It should be noted that the resultant mismatched siRNAs give rise to one nucleotide mismatches against the target mutant allele, and more importantly, two nucleotide mismatches against the wild-type allele (the artificially introduced mismatch and the original variation). Accordingly, we expected that such mismatched siRNAs would exhibit better discrimination between target mutant and wild-type alleles, and only suppress the expression of the mutant alleles.

Effects of mismatched siRNA duplexes on ASP-RNAi against *PRNP-P102L* and *PRNP-P105L* alleles

We selected the siPrnp102(T9) and siPrnp105(T10) duplexes from the first screening of siRNA duplexes against the *PRNP* mutant alleles (Figure 1), and introduced base substitutions into the siRNAs (Figures 2A and E). The resultant mismatched siRNAs were investigated using the assessment system to determine whether they could improve ASP-RNAi. To more precisely determine allele-specific gene silencing, we examined the ratio of the wild-type allele expression to the mutant allele expression. Figures 2B and F show the results of the assessment of the mismatched siPrnp102(T9) and siPrnp105(T10) duplexes, respec-

tively. The results indicate that: (i) introduction of a one-base substitution into the siRNAs was able to influence allele discrimination and RNAi activity, (ii) different nucleotide mismatches appeared to yield different levels of discrimination and inhibition against either the target mutant or wild-type allele, and (iii) some base substitutions appeared to confer marked allele discrimination, resulting in enhancement of ASP-RNAi. It may be of interest that the expression level of the wild-type allele in the presence of siPrnp105(T10)-14U was markedly increased, which may have been caused by the unusual expression level of the control *beta-galactosidase* gene, for as yet unknown reasons. Examination of the ratio of wild-type expression to mutant expression revealed that the siPrnp102(T9)-12C, -13A, -14U and -17G duplexes (Figure 2B) and the siPrnp105(T10)-14U and -15U duplexes (Figure 2F) appear to have markedly improved ASP-RNAi activity. In addition, when HEK293 cells were used instead of HeLa cells, similar results were obtained (data not shown).

To further confirm the results, we examined the effects of the siRNAs on the recognition and inhibition of the *bona fide* wild-type and mutant *PRNP* alleles using their full-length cDNAs. The pPRNPwt-V5 and pPRNPmut102(or mut105)-V5 expression plasmids carrying the wild-type and mutant cDNAs, respectively, were subjected to cotransfection with the siRNAs into HeLa cells, and the expression of the PRNPwt-V5 or the PRNPmut102(or mut105)-V5 polypeptide then examined by Western blotting. The results indicate that while the signal of PRNPwt-V5 in the presence of siPrnp102(T9) or siPrnp105(T10) was reduced, the signal intensity of PRNPwt-V5 was increased in the presence of either siPrnp102(T9)-12C, siPrnp102(T9)-14U or siPrnp105(T10)-15U (Figures 2C and G; supplementary Figure s2A). As expected, the mismatched siRNAs still hold a strong knockdown potency against the mutant *PRNPs* (Figures 2D and H; supplementary Figure s2B). These observations agree with the results for the reporter alleles described above.

Effects of mismatched siRNA duplexes on ASP-RNAi against *PRNP* mutant alleles

From the first screening (Figures 1C and D), we also selected the siPrnp102(T10) and siPrnp178(A9) duplexes and introduced base substitutions into the siRNAs (supplementary Figures s3A and D). Assessment of the mismatched siRNAs suggested that, similar to Prnp102(T9) and Prnp105(T10), introduction of a one-base substitution into the siRNAs influenced ASP-RNAi activity. Furthermore, the ratios of wild-type allele expression to mutant allele expression indicated that the siPrnp102(T10)-13C and siPrnp178(A9)-13C duplexes have significantly improved ASP-RNAi activity (supplementary Figures s3B and E). Western blot analysis indicated that while the PRNPwt-V5 signal was reduced in the presence of either siPrnp102(T10) or siPrnp178(A9), the signal was increased in the presence of the mismatched siPrnp102(T10)-13C or siPrnp178(A9)-13C duplexes (supplementary Figures s3C and F); thus, the data is also compatible with the results for the reporter alleles described above.

Effects of shRNA expression plasmids on ASP-RNAi

As short-hairpin RNA (shRNA) expression vectors appear to be useful for long-term gene silencing [16,27,28], their potential use in ASP-RNAi is also of interest. We constructed shRNA expression plasmids for production of the siPrnp102(T9), (T9)-12C, (T9)-13A, (T9)-14U and (T9)-15U duplexes in cells [designated sh102(T9), sh102(T9)-12C, sh102(T9)-13A, sh102(T9)-14U, sh102(T9)-15U plasmids, respectively]. The shRNA expression plasmids were examined by the assessment system and Western blotting as described above. As shown in Figure 3, the results

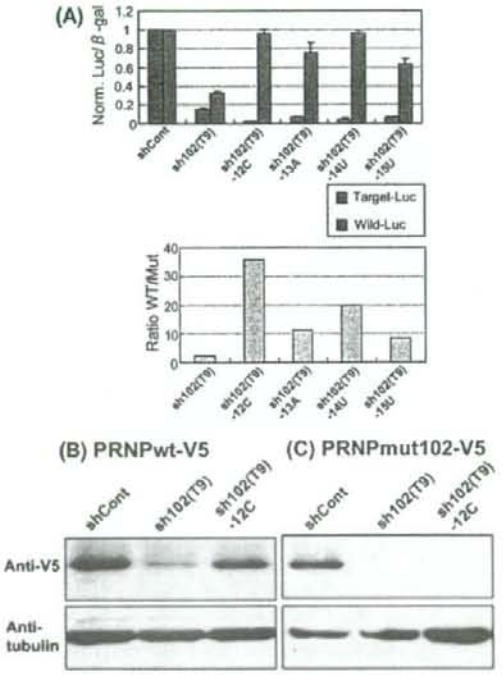

Figure 3. ASP-RNAi with mismatched shRNA expression plasmids against the *PRNP-P102L* mutant. (A) sh102(T9), sh102(T9)-12C, sh102(T9)-14U, sh102(T9)-15U and shCont shRNA expression plasmids for production of siPrnp102(T9), (T9)-12C, (T9)-14U and (T9)-15U duplexes and siControl duplex, respectively, were constructed with reporter alleles and their effects on ASP-RNAi were examined as in Figure 1. Western blot analysis of the wild-type (B) and P102L (C) PRNP polypeptides was carried out as in Figure 2.
doi:10.1371/journal.pone.0002248.g003

indicate that while the sh102(T9) plasmid induced strong gene silencing against either the mutant or wild-type allele, the sh102(T9)-12C, -13A, -14U and -15U plasmids were able to confer allele-specific gene silencing, which agrees with the data for synthetic siRNA duplexes (Figure 2). It is noteworthy that the mismatched shRNA expression plasmids appear to enhance ASP-RNAi to a greater degree than the corresponding synthetic siRNA duplexes; of the mismatched plasmids, the sh102(T9)-12C plasmid, appears to induce strong ASP-RNAi. It is possible that mismatched shRNA expression plasmids are superior to mismatched siRNA duplexes for induction of ASP-RNAi.

Effects of structural modification of siRNA duplexes on ASP-RNAi

In a previous study, we experienced difficulty in inducing ASP-RNAi against the London-type *amyloid precursor protein* (*APP*) mutants, in which single nucleotide substitutions followed by amino acid substitutions (*V717I, V717L, V717G*) were present [17]. While a few designed siRNAs targeting the mutants appeared to discriminate between the mutant and the corresponding wild-type alleles to some degree, most of the siRNAs resulted in weak gene silencing. This is in contrast to the knockdown potency of siRNAs targeting the *PRNP* mutants described above (Figure 1). To

improve such ASP-RNAi, it is necessary to design siRNAs such that they can gain knockdown potency against the mutants, and structural modification may also be applicable for achieving such improvements.

Previous studies showed that fork-siRNA duplexes (F-siRNA duplexes) carrying two nucleotide mismatches at the 3′-ends of the sense-strand siRNA elements are able to enhance RNAi activity to a greater degree than conventional siRNA duplexes [29,30]. Accordingly, we investigated whether F-siRNA duplexes improve ASP-RNAi activity against the London-type *APP* mutants (Figure 4 and supplementary Table s5). The results indicate that several F-siRNA duplexes [F-siAPP(A11), (T11), (G11) and (G12) duplexes] were able to enhance ASP-RNAi to some degree (Figures 4B-D).

In relation to the improvement of ASP-RNAi against the London-type *APP* mutants, we further observed that F-siRNA duplexes, F-siAPP(T12/C13), targeting the Swedish *APP* mutant carrying double nucleotide mutations, were able to markedly improve ASP-RNAi activity, although the conventional siAPP(T12/C13) duplexes induced little or no RNAi activity (Figure 4E).

Different effects of miR-196a and miR-196b on recognition of target *HOXB8*

From the data of the mismatched siPrnp duplexes (Figures 2 and supplementary Figures s2 and s3) and shPrnp RNAs (Figure 3), it appears that the base substitutions conferring marked improvement are largely present in the region of siRNAs corresponding to the seed region of microRNA. This suggests that the region corresponding to the seed region, as well as the central position (where the original variations are present), of guide siRNAs may play a role in allele discrimination in allele-specific gene silencing (details in Discussion). Based on this, it is of particular interest to determine whether the two regions of *bona fide* microRNA (miRNA) can contribute to the regulation of gene expression. From a previous study [31] and an miRNA database, we focused on miR-196a and miR-196b, both of which are nearly complementary to part of the 3′-UTR sequence of *HOXB8* mRNA. Note that one and two mismatches are present in the predicted base-pairing of *HOXB8* with miR-196a and miR-196b, respectively (Figure 5A). In addition, one mismatch, which can form a G:U wobble base-pair, is present in the seed region of both miRNAs, while the other mismatch (U vs. C) is present in the central position of miR-196b. We examined whether the mismatches in miR-196a and miR-196b participate in the recognition of their target, *HOXB8*.

To address this, we constructed a reporter plasmid encoding the *Renilla luciferase* gene with a part of the *HOXB8* sequence in its 3′-UTR. The resultant reporter gene was cotransfected with either synthetic miR-196a or miR-196b duplex into HeLa cells, and the expression levels of the reporter gene then examined. The results (Figure 5B) indicate that miR-196a induced potent inhibition of the expression of the target reporter gene, whereas miR-196b conferred moderate levels of suppression against target reporter gene expression, thus suggesting different levels of recognition against *HOXB8* between miR-196a and miR-196b. Consequently, the evidence suggests that the mismatches in miR-196a and miR-196b probably influence the recognition of their target *HOXB8* mRNA.

Discussion

Enhancement of ASP-RNAi by mismatched siRNAs

In order to realize and control ASP-RNAi, it is necessary to design competent siRNAs or shRNAs possessing strong allele discrimination between target mutant and wild-type alleles, thereby inducing allele-specific gene silencing. In the case of ASP-RNAi, designed siRNAs perfectly match target mutant alleles, but do not correspond with wild-type alleles, i.e., mismatched base pairing(s) will occur at variation site(s) between the siRNAs and wild-type alleles (Figure 6A; wild-type mRNA).

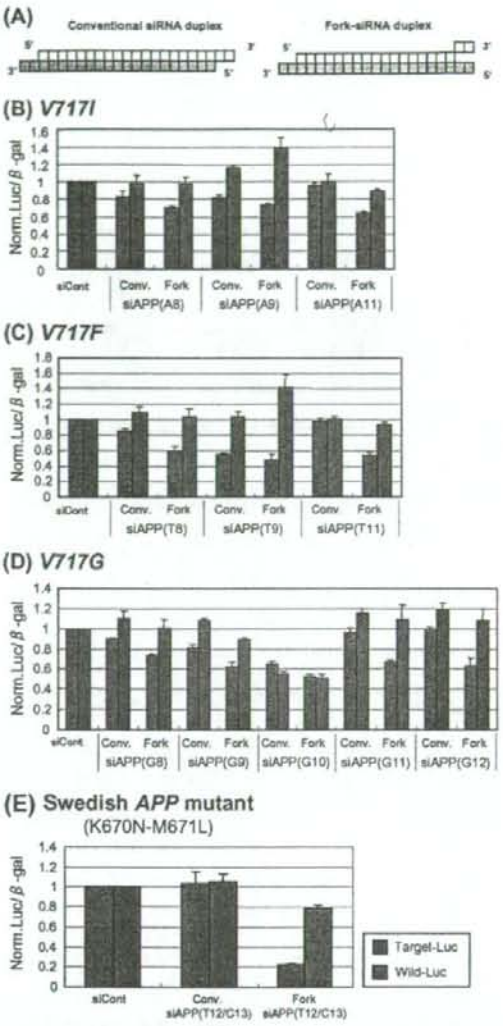

Figure 4. Effects of forked siRNA duplexes on APS-RNAi against *APP* mutants. (A) Schematic drawing of conventional and forked siRNA duplexes. Each box represents a ribonucleotide, and antisense-stranded siRNA elements are indicated by gray boxes. (B)-(E) Comparison of ASP-RNAi activities between conventional (Conv.) and forked (Fork) siRNA duplexes. Assessment of conventional and forked siRNA duplexes against the London *V717I* (B), *V717F* (C), and *V717G* (D) *APP* mutants and the Swedish (E) *APP* mutant was carried out as described previously [17]. The ratios of mutant and wild-type luciferase activities in the presence of siRNA duplexes were normalized against the control ratio obtained in the presence of siControl duplex. Data are averages of at least three independent determinations. Error bars represent standard deviations.
doi:10.1371/journal.pone.0002248.g004

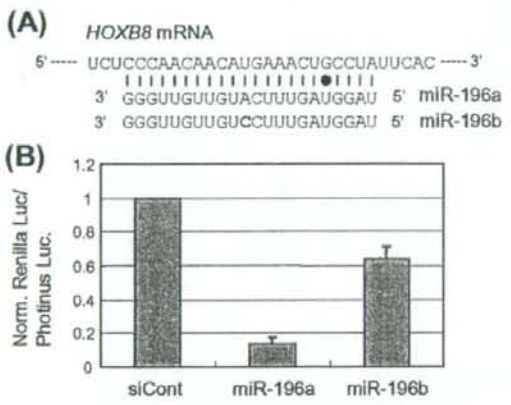

Figure 5. Different knockdown potencies against *HOXB8* between miR-196a and miR-196b. (A) Nucleotide sequences of *HOXB8* mRNA, miR-196a and miR-196b. The *HOXB8* mRNA sequence, which is nearly complementary to miR-196a, together with mature miR-196a and miR-196b are aligned. Perfect base-pairing and G:U wobble base-pairing are indicated by the horizontal bars and dot, respectively. The mismatched base in miR-196b is indicated in red. (B) Effects of miR-196a and miR-196b on gene silencing against *HOXB8*. The miR-196a and miR-196b duplexes were chemically synthesized, as described previously [31]. The synthetic miRNA duplexes, together with a reporter plasmid carrying a part of the *HOXB8* gene (see Materials and Methods), were cotransfected into HeLa cells and the expression of reporter gene was examined. Ratios of normalized target (*Renilla*) luciferase activity to control (*Photinus*) luciferase activity are shown. Data are averages of at least three independent experiments. Error bars represent standard deviations.
doi:10.1371/journal.pone.0002248.g005

Previous studies in which the effects of single-nucleotide mismatches in siRNAs on RNAi activities were systematically examined suggest that nucleotide mismatches are able to influence RNAi activity [26,32]. Our present and previous studies indicate that some, but not all, of the designed siRNA duplexes targeting mutant alleles apparently discriminate the mutant alleles from the wild-type alleles. Since different siRNAs confer different levels of RNAi activity depending upon their thermodynamic properties, the intrinsic knockdown potency may also affect allele discrimination between target and non-target alleles.

In the present study, we observed an improvement in ASP-RNAi when siRNAs induced double knockdown of mutant and wild-type alleles: introduction of a one-base substitution into such siRNAs carrying the original variations around the central position appeared to influence allele discrimination and inhibition of target mutant alleles, although different base substitutions conferred different levels of discrimination and inhibition (Figure 6B). This phenomenon may be associated with the thermodynamic properties of the modified siRNA duplexes. Interestingly, the base substitutions conferring marked ASP-RNAi appeared to be largely present in the region of guide siRNAs, corresponding to the seed region of microRNAs. Since such siRNAs exhibit one and two mismatches against mutant and wild-type alleles, respectively, we suggest that disruption of base-pairing interaction in the seed region, as well as the central position, of the guide siRNAs reduces recognition and/or silencing activity against wild-type alleles, and that a one-base mismatch in the seed region of the guide siRNAs against the target mutant alleles hardly affects gene silencing, i.e., potent RNAi activity against the mutant alleles may remain unchanged.

In addition to the improvement in siRNAs conferring double knockdown of mutant and wild-type alleles, we also observed an enhancement of allele discrimination in ASP-RNAi when siRNAs induced weak knockdown potency, which is in contrast to that of the siRNAs described above. In that case, forked siRNA duplexes carrying two nucleotide mismatches at the 3'-ends of the sense-stranded siRNA elements may allow enhanced allele discrimination between target mutant and wild-type alleles. Since forked siRNA duplexes appear to increase the assembly of antisense-strand (guide) siRNA elements into RISCs, the ease of incorporation of antisense-strand siRNA elements into RISCs may be a key factor for improvement of ASP-RNAi activity.

Altogether, the evidence presented here suggests that structural modification by introduction of base substitution into siRNA or shRNA sequences could influence allele discrimination and silencing activity in ASP-RNAi.

Mismatches in the seed region and the central position of miRNAs affect gene silencing

It is noteworthy that destabilization of base-pairing interaction in the seed region, as well as in the central position, of *bona fide* miRNAs appears to also influence recognition and/or suppression of target RNAs. In the case of miR-196a and miR-196b presented in this study, the miRNAs appear to induce different levels of suppression against *HOXB8* RNA. Accordingly, it is conceivable that the difference in gene silencing involving miRNAs could yield complex regulation of gene expression. Since there are various base-pairing interactions between miRNAs and their target RNAs, such interactions may contribute in the generation of various and complex gene regulatory events. More extensive research is required to further evaluate this possibility.

Properties of siRNA duplexes conferring ASP-RNAi

Based on the assessed siRNA duplexes efficacy of ASP-RNAi, it appears that different siRNA duplexes induce different levels of ASP-RNAi, suggesting that allele-specific knockdown potencies are most likely dependent on the designed siRNA sequences. Previous studies have suggested that functional siRNA duplexes can be characterized by low base-pairing stability at their 3'-ends [29,33–35], i.e., an asymmetrical feature of base-pairing stability occurs between both ends of functional siRNA duplexes. From the alignment of the siRNA sequences examined in the present and previous studies, it was observed that the siRNA duplexes conferring little or no gene silencing possessed symmetrical base-pairing stability and contained G or C residues at many 3'-ends of their sense-stranded elements (supplementary Table s7A): these features are distinct from those of functional siRNA duplexes. In contrast to the above siRNA duplexes, most of the siRNA duplexes triggering strong RNAi activity, including ASP-RNAi, tended to have asymmetrical base-pairing stability (supplementary Table s7B). It may be of interest to elucidate the properties of siRNA duplexes that confer strong ASP-RNAi, other than the asymmetrical feature. To address this, extensive examination of the knockdown potency of siRNA duplexes targeting various mutant alleles is required.

In conclusion, in order to realize ASP-RNAi against target mutant alleles carrying nucleotide variations, the design and evaluation of competent siRNA duplexes conferring ASP-RNAi is vital; but designed siRNAs do not always confer potent ASP-RNAi activity. The evidence presented here suggests that structural modification of siRNA duplexes by base substitutions may improve ASP-RNAi. The key regions in an siRNA duplex for such modifications are the central position, the seed region and the 3'-end of the sense-strand siRNA element, which appear to be related to target RNA cleavage, target RNA recognition and assembly of the antisense-strand (guide)

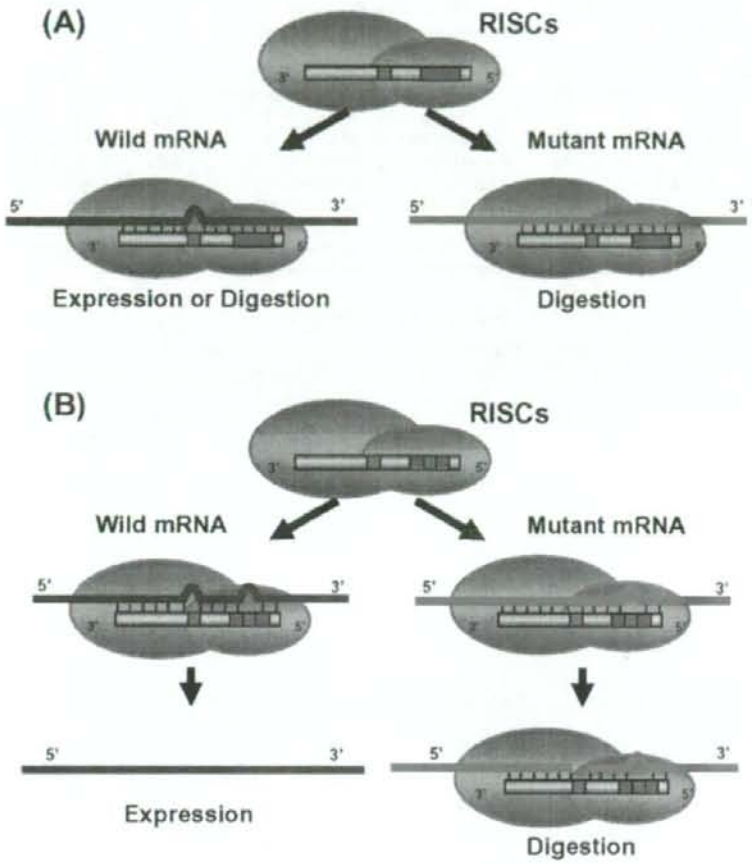

Figure 6. Schematic summary of allele-specific gene silencing with mismatched siRNA. Guide siRNA elements in RISCs are indicated by gray bars, in which nucleotide variation and the seed region are indicated by red and blue boxes, respectively. Introduced base substitutions are indicated by green boxes. Mutant and wild-type allelic transcripts are indicated by red and blue lines, respectively. (A) When designed siRNA targeting the mutant allele has potential for potent gene silencing, not only the mutant but also the wild-type alleles may be inhibited by RNAi mediated by the siRNA, i.e., double knockdown against both alleles may occur. (B) When a one-base substitution is introduced into the seed region of an siRNA conferring double knockdown, the resultant (guide) siRNA generates one and two mismatches against the mutant and wild-type alleles, respectively, thereby possibly gaining the ability to induce ASP-RNAi.
doi:10.1371/journal.pone.0002248.g006

siRNA element into RISCs, respectively. Therefore, structural modification of such functional portions of siRNA duplexes may greatly influence allele discrimination and gene silencing activity, thereby conferring improvement of ASP-RNAi.

Materials and Methods

Preparation of oligonucleotides

RNA and DNA oligonucleotides were obtained from TAKARA BIO, and INVITROGEN or BEX, respectively. For preparation of duplexes, sense- and antisense-strand oligonucleotides (20 μM each) were mixed and annealed, as described previously [29]. Sequences of synthesized RNA and DNA oligonucleotides are shown in supplementary Tables s1, s2, s3, s4, s5 and s6. Non-silencing siRNA duplex (siControl; Qiagen) was used as the negative control.

Cell culture

HeLa and HEK293 cells were grown at 37°C in Dulbecco's modified Eagle's medium (Wako) supplemented with 10% fetal bovine serum (Sigma), 100 U/ml penicillin and 100 μg/ml streptomycin (Wako) in a 5% CO_2-humidified chamber. HEK293 cells (Registry No. JCRB9068) were obtained from the Health Science Research Resources Bank.

Construction of reporter alleles and shRNA expression plasmids

Reporter alleles were constructed as described previously [17]. Briefly, phRL-TK (Promega) and pGL3-TK [30] plasmids encoding the *Renilla* and *Photinus luciferase* genes, respectively, were digested with XbaI and NotI, and subjected to ligation with synthetic oligonucleotide duplexes corresponding to the *PRNP*-

P102L, *PRNP-P105L* and *PRNP-D178N* alleles, as well as wild-type alleles (oligonucleotide sequences are indicated in supplementary Table s3). The resultant plasmids carry allelic *PRNP* sequences in the 3′-untranslated regions (UTRs) of the *luciferase* genes (Figure 1A). The London-type *APP* mutant and wild-type *APP* reporter alleles described in a previous paper [17] were also used. For construction of shRNA expression vectors, the GeneSilencer shRNA Vector (Gene Therapy System, Inc.) was used, and synthetic oligonucleotide duplexes were inserted into the vector according to the manufacturer's instructions (oligonucleotide sequences are indicated in Table s4). To construct a reporter plasmid carrying part of the *HOXB8* sequence, psiCHECK-2 vector (Promega) was digested with XhoI and PmeI, and subjected to ligation with synthetic *HOXB8* oligonucleotide duplex (supplementary Table s3). With regard to expression plasmids carrying a full-length cDNA of the human *PRNP* linked with the V5-tag sequence, the wild-type *PRNP* cDNA was amplified by RT-PCR with human brain total RNA (Ambion), trimmed with EcoRI and NotI, and inserted into the pTracer-EF/Bsd vector (Invitrogen); the resultant plasmid was designated 'pPRNPwt-V5'. Using this plasmid, mutant plasmids carrying the *PRNP P102L* and *P105L* were constructed using the GeneEditor *in vitro* Site-Directed Mutagenesis System (Promega) and the QuikChange Site-Directed Mutagenesis Kit (Stratagene), respectively, according to the manufacturer's instructions; the resultant mutant expression plasmids were designated 'pPRNPmut102-V5' and 'pPRNPmut105-V5'. The PCR primers for *PRNP* cDNA synthesis and oligonucleotides used for the mutagenesis were as follows:

For *PRNP* cDNA synthesis;

Forward PCR primer; 5′-TTCCGAATTCGCCACCATGGCGAACCTTGGCTGCT-3′

Reverse PCR primer; 5′-ACATTGCGGCCGCTCCCACTATCAGGAAGATGAGG-3′

For site-directed mutagenesis:

PRNP P102L oligo DNA;

5′-pGTGGAACAAGCTGAGTAAGCCAA-3′

PRNP P105L oligo DNAs;

Forward;

5′-GGAACAAGCCGAGTAAGCTAAAAACCAACATGAAGCACATGGC-3′

Reverse;

5′- GCCATGTGCTTCATGTTGGTTTTTAGCTTACTCGGCTTGTTCC-3′

Transfection and reporter assay

The day before transfection, cells were trypsinized, diluted with fresh medium without antibiotics, and seeded into 24-well culture plates (approximately 0.5×10^5 cells/well). Next, 0.24 μg (40 nM) of siRNA duplexes or 0.1 μg of shRNA vectors together with 0.2 μg of pGL3-TK-backbone plasmid, 0.05 μg of phRL-TK-backbone plasmid and 0.1 μg of pSV-β-Galactosidase control vector (Promega) as a control were applied to each well using Lipofectamine 2000 transfection reagent (Invitrogen) as described previously [30]. Twenty-four hours after transfection, cell lysate was prepared and expression levels of luciferase and β-galactosidase were examined using the Dual-Luciferase reporter assay system (Promega) and Beta-Glo assay system (Promega), respectively, according to the manufacturer's instructions. The luminescent signals were measured using a TD-20/20 luminometer (Promega).

Western blotting

The pPRNPwt-V5 or pPRNPmut102(or mut105)-V5 plasmid (0.1 μg) was cotransfected with siRNA duplex (0.24 μg) or shRNA expression plasmid (0.1 μg) into HeLa cells. Forty-eight hours after transfection, cell lysate was prepared and examined by Western blotting. Equal amounts of cell lysate were separated by SDS-PAGE and electrophoretically blotted onto PVDF membranes (Millipore). Membranes were blocked for 1 h in blocking solution [5% non-fat milk in washing buffer (0.1% Tween-20 in PBS)] and incubated with anti-V5 antibody (Invitrogen) or anti-α-tubulin antibody DM1A (Sigma), followed by washing in PBS containing 0.1% Tween-20 and further incubation with horseradish peroxidase-conjugated donkey anti-mouse IgG (Jackson ImmunoResearch Laboratories). Antigen-antibody complexes were visualized using Immobilon Western reagent (Millipore). The experiments were duplicated at least twice independently.

Supporting Information

Figure S1 Wild-type and mutant PRNP mRNAs and designed sense-strand siRNAs. The wild-type and mutant PRNP mRNA sequences around the P102L (A), P105L (B), and D178N (C) variations, respectively, are shown and the nucleotide variations are indicated in red. Designed siRNAs (indicated) are represented by thin lines and only the variations are indicated in red.
Found at: doi:10.1371/journal.pone.0002248.s001 (0.26 MB TIF)

Figure S2 Expression of the wild-type (A) and P102L (B) PRNP polypeptides in the presence of indicated siRNAs was examined by Western blotting as in Figure 2. Expression of alpha-tubulin was also examined as the control.
Found at: doi:10.1371/journal.pone.0002248.s002 (0.99 MB TIF)

Figure S3 Assessment of mismatched siPrnp102(T10) and siPrnp178(A9) on ASP-RNAi. (A, D) Nucleotide sequences of wild-type and mutant PRNP mRNAs and designed siRNAs are indicated as in Figure 2. (B, E) Assessment of mismatched siRNAs was carried out and the results are shown as in Figure 2. (C, F) Western blot analysis of the wild-type PRNP polypeptide (PRNPwt-V5) in the presence of indicated siRNAs was carried out as in Figure 2. The PRNPwt-V5 gene was driven by the EF-1α promoter instead of the CMV promoter in this experiment. Expression of α-tubulin was also examined as the control.
Found at: doi:10.1371/journal.pone.0002248.s003 (0.61 MB TIF)

Table S1
Found at: doi:10.1371/journal.pone.0002248.s004 (0.04 MB DOC)

Table S2
Found at: doi:10.1371/journal.pone.0002248.s005 (0.05 MB DOC)

Table S3
Found at: doi:10.1371/journal.pone.0002248.s006 (0.03 MB DOC)

Table S4
Found at: doi:10.1371/journal.pone.0002248.s007 (0.03 MB DOC)

Table S5
Found at: doi:10.1371/journal.pone.0002248.s008 (0.04 MB DOC)

Table S6
Found at: doi:10.1371/journal.pone.0002248.s009 (0.03 MB DOC)

Table S7
Found at: doi:10.1371/journal.pone.0002248.s010 (0.11 MB DOC)